Geological Magazine

www.cambridge.org/geo

Original Article

Cite this article: Aguirre-Díaz GJ, Coutiño-Taboada ME, Ubach-Cozatl ME, Martí J, Martínez-Reyes JJ, Tristán-González M, Solari LA, and Pielli-Espinosa F. The Guanajuato resurgent graben caldera, Sierra Madre Occidental, central México: revised volcanic stratigraphy and geologic evolution. *Geological Magazine* **162**(e26): 1–25. https://doi.org/10.1017/S0016756825100071

Received: 9 May 2024
Revised: 10 May 2025
Accepted: 30 May 2025

Keywords:
Resurgent graben-caldera; volcanic stratigraphy; volcano-tectonics; mid-Tertiary ignimbrites; Sierra Madre Occidental; Guanajuato

Corresponding author:
Gerardo J. Aguirre-Díaz;
Email: ger@geociencias.unam.mx

CAMBRIDGE UNIVERSITY PRESS

The Guanajuato resurgent graben caldera, Sierra Madre Occidental, central México: revised volcanic stratigraphy and geologic evolution

Gerardo J. Aguirre-Díaz[1], Mariana E. Coutiño-Taboada[2], María Eugenia Ubach-Cozatl[3], Joan Martí[4], Juan José Martínez-Reyes[2], Margarito Tristán-González[5], Luigi A. Solari[1] and Franco Pielli-Espinosa[6]

[1]Instituto de Geociencias, Universidad Nacional Autónoma de México, Campus Juriquilla, Querétaro, México; [2]Escuela de Minas, Universidad Autónoma de Guanajuato, Guanajuato, México; [3]Ciencias de la Tierra, Facultad de Ciencias, Universidad Nacional Autónoma de México, Ciudad de México, México; [4]Geociencias, Instituto de Diagnóstico Ambiental y Estudios Agua, Consejo Superior de Investigaciones Científicas (CSIC), Barcelona, Spain; [5]Instituto de Geología, Universidad Autónoma de San Luis Potosí, San Luis Potosí, México and [6]Ciencias de la Tierra, UMDI-FC-Juriquilla, Universidad Nacional Autónoma de México, Ciudad de México, México

Abstract

The Guanajuato Mining District of central Mexico is one of the main silver and gold deposits in the world. It is in the State of Guanajuato in the southern part of the Sierra Madre Occidental (SMO) volcanic province. The mining district developed within a mid-Tertiary volcano-sedimentary sequence that includes thick alluvial-fan deposits accumulated in a tectonic basin during the Eocene-Oligocene named the Guanajuato Red Conglomerate and an overlying volcanic sequence mostly pyroclastic of Oligocene age. The mid-Tertiary stratigraphy of Guanajuato is revised and reinterpreted in the light of new fieldwork and U-Pb ages, which document a close timing between all units of the volcanic succession at the top of the Guanajuato Red Conglomerate. This sequence is made of pyroclastic density current deposits formed during episodic events from the Guanajuato caldera. A new nomenclature of the caldera's units is proposed; the Guanajuato Caldera Volcanic Group, which includes the Guanajuato Pyroclastic Formation represented by the Loseros PDC deposits and the Bufa-Calderones ignimbrites emplaced around 32.8 ± 0.2 Ma, and the post-collapse lava domes of El Rodeo and Chichíndaro formations emplaced at 31–30 Ma. Apparently, a resurgent pulse of the caldera uplifted the collapsed intra-caldera blocks, so that the caldera floor is now exposed. The caldera collapse was controlled by the pre-existing normal faults inherited from the previous tectonic basin; thus, it is classified as a graben-type caldera, with a square shape and a size of 15 × 16 km. By comparison with other similar calderas of Mexico, the Guanajuato caldera is another case study of graben-type calderas of the SMO coinciding with mineral districts, such as Bolaños (Jalisco).

1. Introduction

The Sierra Madre Occidental (SMO) is a continental margin volcanic province characterized by voluminous silicic ignimbrites that accumulated thicknesses of 500 to 1500 m (McDowell & Clabaugh, 1979; Aguirre-Díaz *et al.* 2008; Fig. 1a). This ignimbrite sequence formed mostly within 38–22 Ma, building up a total estimated volume of ca. 580,000 km^3, making the SMO the largest ignimbrite province of the world (Aguirre-Díaz & Labarthe-Hernández, 2003). It has been proposed that several and probably most of the SMO ignimbrites erupted from fissures associated with Basin and Range fault systems or graben (Aguirre-Díaz & Labarthe-Hernández, 2003), thus, referring to several of these volcano-tectonic structures as graben calderas (Aguirre-Díaz, 2008; Aguirre-Díaz *et al.* 2008).

The Guanajuato graben caldera is in central Mexico, about 280 km to the NW of Mexico City, and forms part of the SMO Volcanic Province (Fig. 1a, c). The caldera is within the economically important mining district of Guanajuato, with 28 silver and gold mines, some active since the 16th century (Echegoyén-Sánchez *et al.* 1970; Mango *et al.* 1991; Randall *et al.* 1994; Orozco-Villaseñor, 2014; Vassallo, 2018). With a historic production of 37,000 metric tonnes of silver and 135 of gold, the Guanajuato Mining District has been one of the most important precious metal producers in the world (Orozco-Villaseñor, 2014). Nieto-Samaniego *et al.* (2016) propose a relationship between the ore deposits with a volcanic structure in Guanajuato, suggesting a caldera. However, further geologic, geochronologic and trace-element geochemical work is necessary due to the important economic implications and the potential role of Guanajuato as

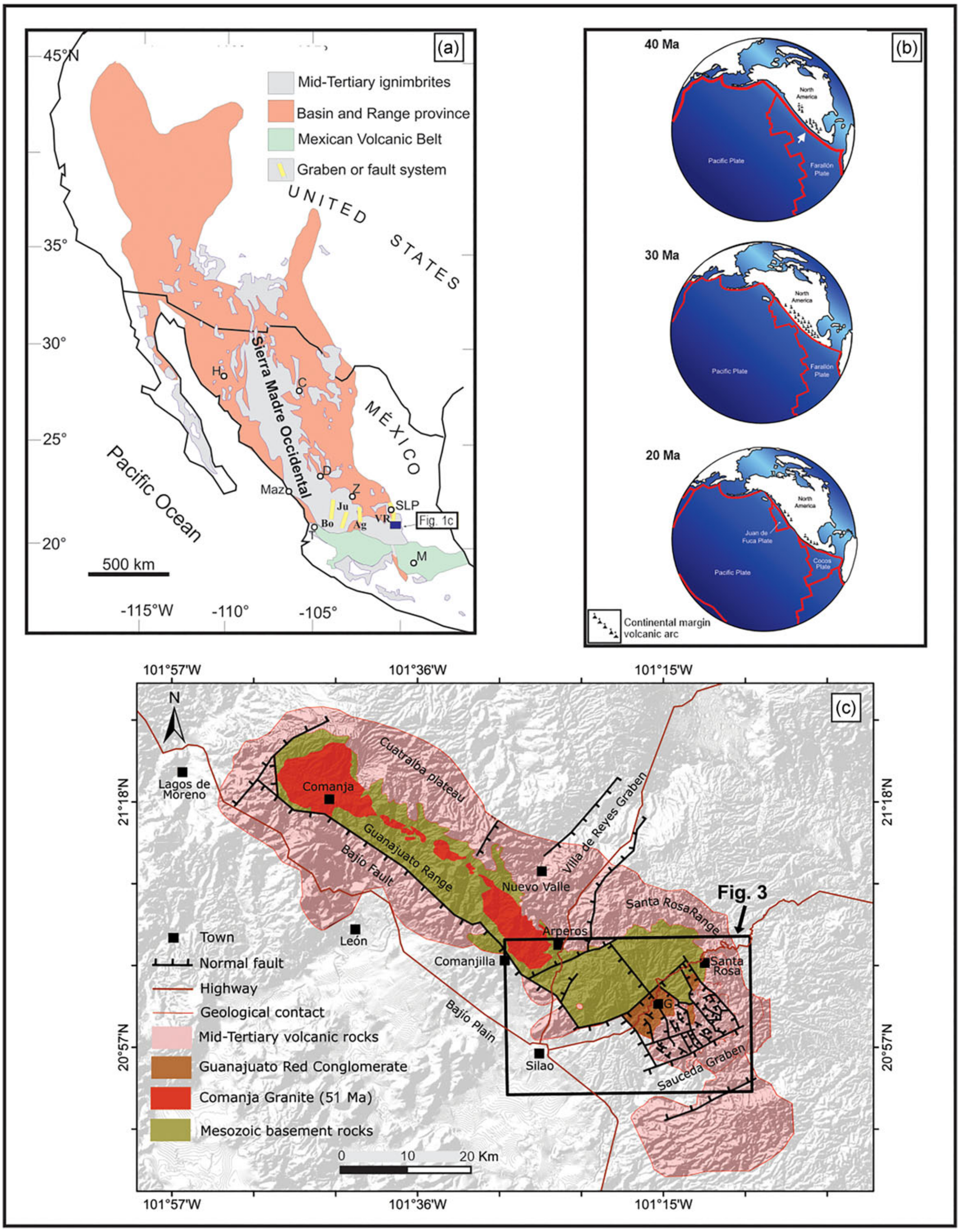

Figure 1. Index maps. (a) Regional map of the Sierra Madre Occidental volcanic province and the Basin and Range tectonic province, indicating the location of the study area (black square with label Fig. 1c) and features mentioned in text; cities: M-Mexico, SLP-San Luis Potosí, Z-Zacatecas, T-Tepic, Maz-Mazatlán, D-Durango, C-Chihuahua, H-Hermosillo; graben: Bo-Bolaños, Ju-Juchipila, Ag-Aguascalientes, VR-Villa de Reyes (modified from Aguirre-Díaz & Labarthe-Hernández, 2003). (b) Plate tectonic configuration for the Farallon subducted plate beneath the North American plate for the 40 to 20 Ma timing, which generated the mid-Tertiary continental margin volcanic arc that resulted in the Sierra Madre Occidental volcanic province. Modified from Atwater (1989, 2022) for the tectonic framework, and Aguirre-Díaz and McDowell (1991) and Ferrari *et al.* (1999) for the volcanic arc patterns. (c) Local index map showing the Guanajuato Range in central Mexico with main geological features (modified from Randall *et al.* 1994 and Coutiño-Taboada, 2015). Rectangle marks the map of the study area shown in Figure 3.

analogue for the exploration and exploitation of similar ore districts in the SMO or in other places.

The idea that there is a caldera structure in Guanajuato dates to Randall *et al.* (1994), who mention that several Cenozoic volcanic units in the Guanajuato area are probably related to a caldera, such as La Bufa and Calderones formations. Aranda-Gómez *et al.* (2003, 2012) agree that some of the major pyroclastic units are pyroclastic rocks instead of sedimentary rocks as previously thought, such as the Calderones Formation. Aguirre-Díaz *et al.* (2012*a*, 2012*b*, 2013*a*, 2013*b*, 2014) and the thesis work by Coutiño-Taboada (2015) revised the mid-Tertiary volcanic sequence in the Guanajuato Mining District and documented it with isotopic ages, concluding that there is a graben-type caldera at Guanajuato that was related to the regional tectonic normal faults in the area following the caldera classification of Aguirre-Díaz (2008). Therefore, Guanajuato caldera and its products should be part of the SMO calderas and related ignimbrites associated with the Basin and Range extensional tectonics (Aguirre-Díaz & Labarthe-Hernández, 2003; Aguirre-Díaz *et al.* 2008). Nieto-Samaniego *et al.* (2016) confirm the evidence of a fault-controlled volcanic centre at Guanajuato, providing similar ages as those reported by Coutiño-Taboada (2015) and Aguirre-Díaz *et al.* (2016).

The results obtained can be useful to compare with other similar graben caldera structures, such as Ilopango at El Salvador (Suñe-Puchol *et al.* 2019*a*, 2019*b*), Cañas Dulces at Costa Rica (Molina-Zúñiga *et al.* 2014), calderas at the Catalan Pyrenees (Martí, 1991; Martí *et al.* 2018, 2024; Saura *et al.* 2025), the Bolaños mining district at Mexico (Aguirre-Díaz *et al.* 2021) and other volcano-tectonic structures in other sites of the SMO (Aguirre-Díaz & Labarthe-Hernández, 2003; Aguirre-Díaz *et al.* 2008; Tristán-González *et al.* 2008), contributing to advance on the knowledge of the dynamics of the tectonically controlled collapse calderas and the occasional relation that such volcanic structures have with mineral deposits of high economic interest, as in the Guanajuato and Bolaños mining districts.

2. Previous works: geologic setting of the Guanajuato caldera

The Sierra de Guanajuato is part of the SMO volcanic province (Fig. 1), close to the northern border of the Mexican Volcanic Belt (MVB) province. Other authors include it in the Mesa Central province of Mexico (Nieto-Samaniego *et al.* 1996, 2016; Tristán-González *et al.* 2009), but we prefer to use the definition of Aguirre-Díaz and Labarthe-Hernández (2003) for the SMO regarding it as a volcanic province, or volcanic field, in which it is extended beyond the physiographic province to the central portion of Mexico. SMO and MVB are the largest volcanic provinces of Mexico, which evolved with time to end up having an 'L' shape distribution pattern on a map view (Fig. 1a; Ferrari *et al.* 1999). The SMO was linked to the tectonics of the extinct Farallon plate subduction beneath North America (Fig. 1b; Atwater, 1989; McDowell & Clabaugh, 1979; Aguirre-Díaz & McDowell, 1991; Ferrari *et al.* 1999; Andrews *et al.* 2022), and the MVB to the subduction of smaller oceanic plates Rivera and Cocos that are remnants of the Farallon plate (Fig. 1b), subduction that is still active along the Middle American Trench, forming part of the Pacific Ring of Fire (Nixon, 1982; Aguirre-Díaz *et al.* 1998; Siebe *et al.* 2006). The SMO Ignimbrite Flare-up took place from about 38 to 22 Ma (Aguirre-Díaz *et al.* 2008) and overlapped in space and time with the Basin and Range extension (Aguirre-Díaz & Labarthe-Hernández, 2003), with episodic peaks of both ignimbrite-forming eruptions and extension. Therefore, most of the large volume of the Ignimbrite Flare-up apparently erupted from Basin and Range fault-related fissures that resulted in graben-type calderas (Aguirre-Díaz & Labarthe-Hernández, 2003; Aguirre-Díaz *et al.* 2008).

From the Guanajuato Mining District area and northward until the US-Mexico border, there are Oligocene volcanic rocks related to the SMO for about 1500 km (Fig. 1a), whereas to the south, there is a predominance of Miocene-Pliocene rocks of the MVB (Cerca-Martínez *et al.* 2000). The Guanajuato Range (Fig. 1c) includes three main sequences (Fig. 2); (1) the basement complex formed of Mesozoic to earliest Tertiary rocks related to a terrane accretion origin, the Guerrero Terrane (Campa & Coney, 1983; Monod *et al.* 1990; Centeno-García *et al.* 2008; Ortega-Gutiérrez *et al.* 2008), characterized by slightly metamorphosed but intensely deformed volcano-sedimentary rocks and several arc-related intrusive bodies of diverse compositions and ages (Campa & Coney, 1983; Monod *et al.* 1990; Ortiz-Hernández *et al.* 1990; Martínez-Reyes, 1992; Lapierre *et al.* 1992; Sedlock *et al.* 1993; Randall *et al.* 1994; Miranda-Avilés *et al.* 2016); (2) the Comanja granite, a massive pluton of batholitic size and stratigraphically between the two main sequences (Martínez-Reyes, 1992; Quintero, 1992), and dated at 51 ± 0.3 to 49.5 ± 0.8 Ma using U/Pb zircon ages (del Rio *et al.* 2020); and (3) the 'cover rocks', a mid-Tertiary sequence unconformably overlaying or in fault contact with the basal complex. This younger sequence consists of 1,500–2,000 thick mid-Tertiary continental clastic sediments (the Guanajuato Red Conglomerate Formation), and volcanic rocks including rhyolitic and dacitic tuffs and rhyolitic, dacitic and mafic-andesitic lavas (Edwards, 1955; Echegoyén-Sánchez *et al.* 1970; Martínez-Reyes, 1992; Randall *et al.* 1994; Nieto-Samaniego *et al.* 1996, 2016; Cerca-Martínez *et al.* 2000; Aranda-Gómez *et al.* 2003, 2012; Aguirre-Díaz *et al.* 2012*a*, 2012*b*, 2014; Coutiño-Taboada, 2015; Puy-Alquiza *et al.* 2017).

The presence of a caldera structure at the Guanajuato City area was already inferred since studies conducted in the area in the 1990s (Aranda-Gómez *et al.* 2003; Randall *et al.* 1994). However, the study area was affected by extensional tectonics and uplifting during the mid-Tertiary time (Nieto-Samaniego *et al.* 2007; Tristán-González *et al.* 2008); and it was deeply eroded, so extra-caldera units are sparse, but intra-caldera units are still preserved. Randall *et al.* (1994) proposed the existence of a caldera structure limited by a semicircular ring fracture, in which at its interior there is a thick volcano-sedimentary succession. Further studies by our group (Aguirre-Díaz *et al.* 2012*a*, 2012*b*, 2013*a*, 2013*b*, 2014; Coutiño-Taboada, 2015; Ubach-Cozatl, 2023; Ubach-Cozatl & Aguirre-Díaz, 2023) confirm the existence of the Guanajuato caldera, but as a graben type (Fig. 3). In this work, we describe the pyroclastic units that are related to the collapse of the Guanajuato caldera, the post-collapse felsic lavas and a probable resurgence event of the caldera, which has not been proposed in previous works, and it is important for understanding the exposure of the caldera floor.

3. Methodology

In this paper, we present a revision of the stratigraphic nomenclature of the Guanajuato Mining District and a volcanic evolution model for the Guanajuato graben caldera and its volcanic phases. The evolution model and conclusions are based on fieldwork (geologic mapping, stratigraphy, physical volcanology and structural geology), U-Pb zircon ages and mineral characterization (petrographic analyses) to infer the chemical classification of the sequence, as rocks are highly and pervasively altered by hydrothermalism and weathering for reliable whole-rock major element chemistry. We revise and describe the stratigraphy and age of the caldera succession and the tectonic structure of the caldera

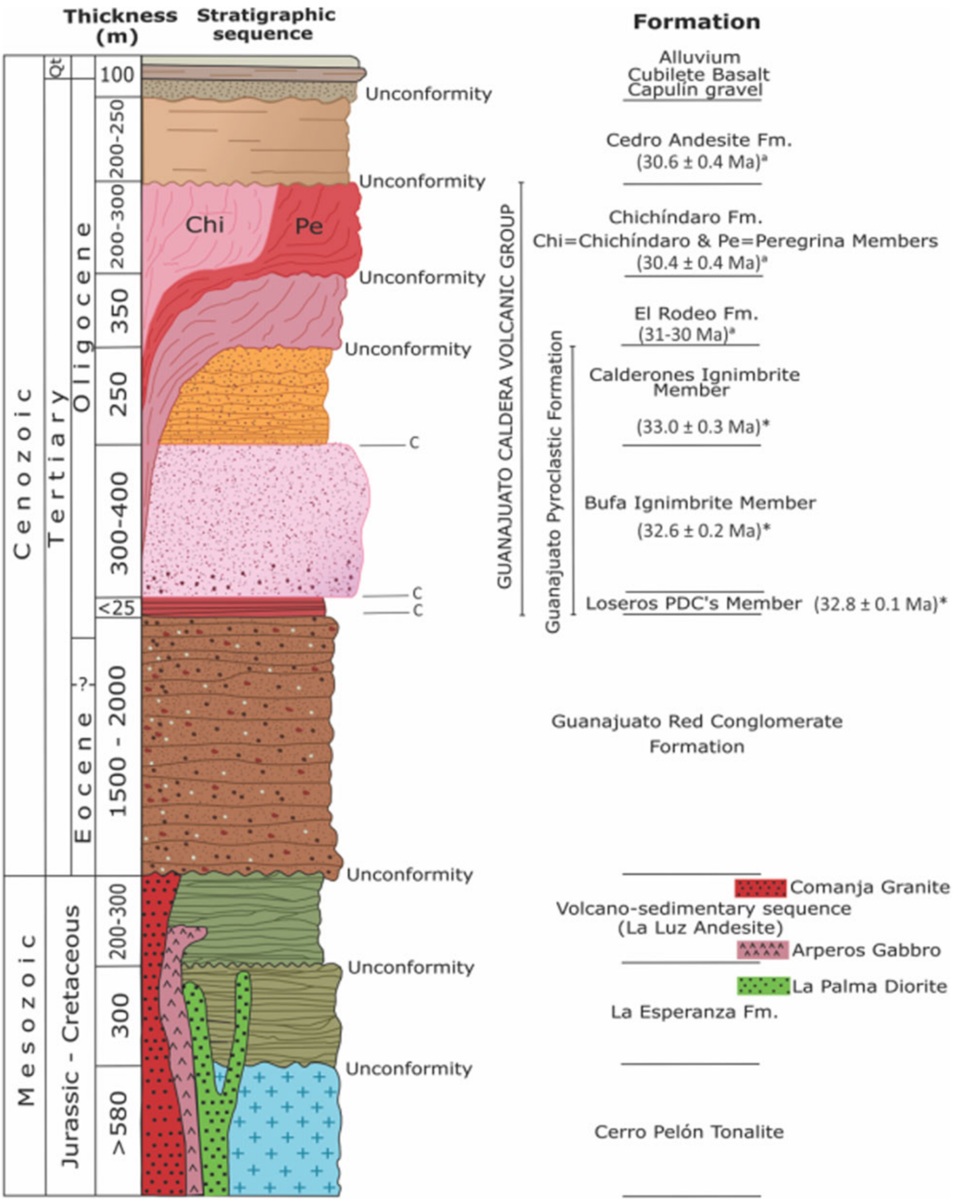

Figure 2. Composite stratigraphic section of the study area with the new nomenclature for the units of the Guanajuato Caldera Volcanic Group. Isotopic ages: [a]age of other authors (Table 1); *age reported in this work (Table 2). Modified after Randall *et al.* (1994).

depression. By integrating all the data available, we construct a conceptual model on the formation and development of the Guanajuato caldera, which was controlled by a pre-existing graben.

3.a. Fieldwork

Fieldwork for this study has been undertaken since 2014 during the thesis work of Coutiño-Taboada (2015). Field campaigns lasted generally 1 to 2 weeks, for a total of about 150 days during which the co-authors that signed this work participated. We collected about 300 rock samples. We followed standard fieldwork techniques, including the use of aerial photographs, orthophotos and satellite images, measurement of stratigraphic sections, bedding and faults, recognition of unconformities and disconformities, and rock sampling under strict stratigraphic control. We used previous maps already published in the area as starting point; particularly those of Edwards (1955), Echegoyén-Sánchez et al. (1970), Martínez-Reyes (1992), Randall *et al.* (1994), and the Mexican Geological Service (Servicio Geológico Mexicano, 2023). The lithostratigraphic units were defined following the recommendation of Martí *et al.* (2018) for volcanic systems. Topographic maps of the Mexican geographic agency INEGI (2023) were used as base maps, both as printed copies and as digital files for their use in a Geographic Information System (GIS), in this case, the QGIS software.

3.b. U-Pb geochronology

A total of 6 isotopic ages were performed for this study. Results are presented in Section 5. The procedure includes zircon separation from felsic rocks using a hydraulic piston crusher and sieving to obtain the 60–80 mesh fraction. Zircon and other heavy minerals were washed and separated using a pan; zircons were later separated by hand-picking using a binocular microscope. The selected crystals were mounted on a glass slide using adhesive tape. A briquette was later prepared with epoxy resin and was polished.

https://doi.org/10.1017/S0016756825100071 Published online by Cambridge University Press

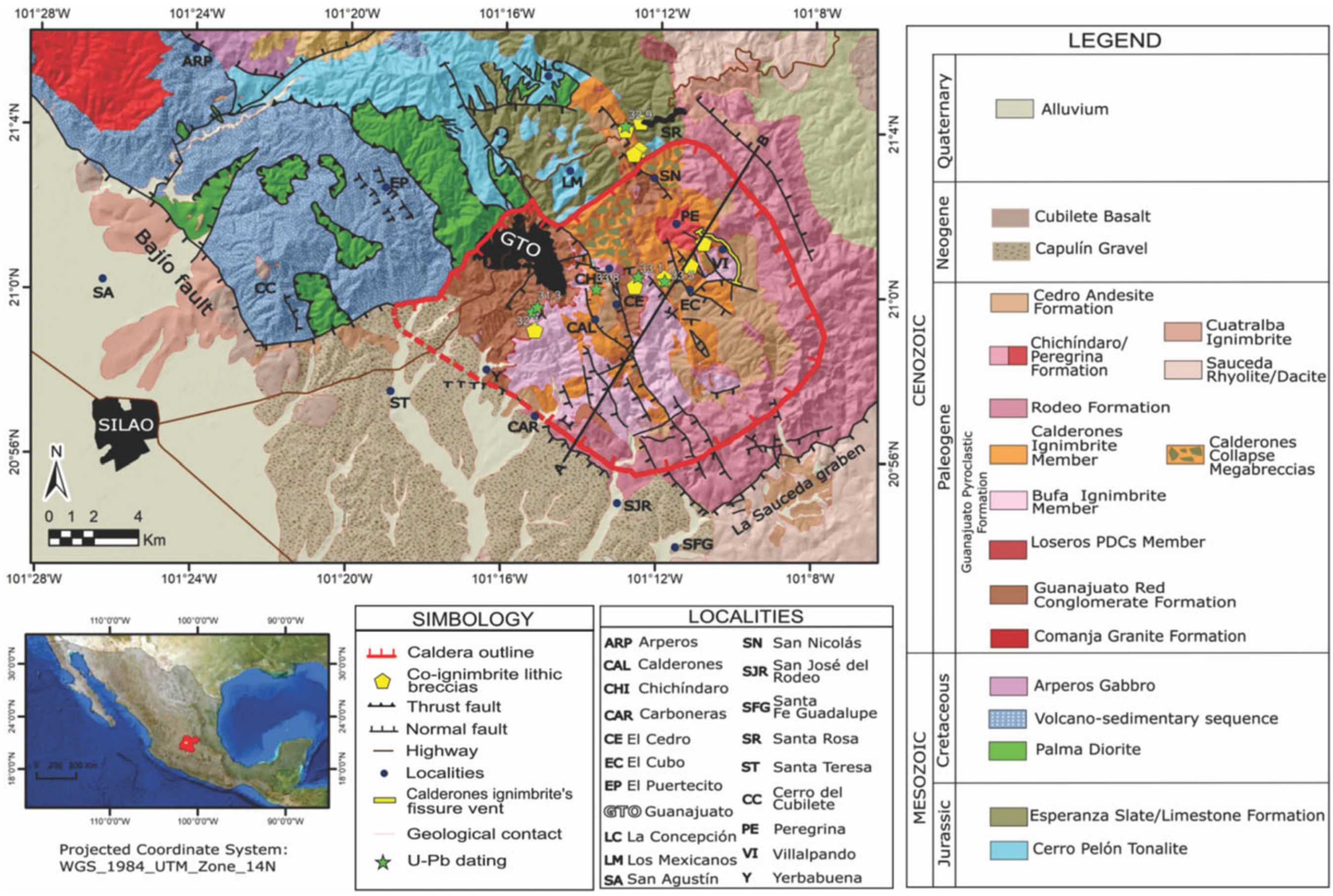

Figure 3. Geological map of the Guanajuato graben caldera and surrounding area, indicating sites for isotopic ages reported in this work and co-ignimbrite lithic breccias. Line A-B corresponds to the geological cross section shown in Figure 17.

U-Pb isotope measurements were performed by laser ablation ICP-MS at the Laboratorio de Estudios Isotópicos, Instituto de Geociencias, Universidad Nacional Autónoma de México, using a Thermo ICap Qc quadrupole mass spectrometer coupled to a Resolution M050, 193 nm excimer laser ablation workstation. A 23-µm spot was employed, with a repetition rate of 5 Hz and a 6 J/cm-2 of fluence, following the analytical procedures described in Solari *et al.* (2018). The standard zircon 91,500 (1065.4 +/− 0.6 Ma, TIMS age, Wiedenbeck *et al.* 1995) was employed as a primary standard. Plešovice standard zircon (337.13 +/− 0.37 Ma, TIMS age, Sláma *et al.* 2008) was employed as a control standard, yielding during the current analytical session a concordant age of 339.4 +/− 1.5 Ma (n = 15, MSWD = 1.4), in agreement with its accepted age. Data processing was performed offline using Iolite software v. 4.5 (Paton *et al.* 2010) and the Vizual-Age data reduction scheme of Petrus and Kamber (2012). No common Pb correction was applied since the 204Pb signal (non-radiogenic Pb) is swamped by the isobar 204Hg. Data were exported from Iolite and the concordia diagrams and mean ages were calculated using IsoplotR (Vermeesch, 2018). The calculated age uncertainties are 2-sigma. The analytical procedure is described in Solari *et al.* (2018). Data processing for age calculation was done using the IsoplotR tool (Vermeesch, 2018).

3.c. Petrographic analyses

About 50 representative samples were prepared for petrographic inspection with the microscope. Thin sections were done in the workshops of the Geosciences Institute of UNAM following the standard procedure for sample handling and thin section preparation. A petrographic research microscope, Nikon Labophoto 2- POL, was used for textural analyses, which was coupled to a Nikon camera for obtaining high-quality digital photomicrographs.

4. Results of this work

4.a. Stratigraphy of the Guanajuato caldera revised as a volcanic system

Since Guanajuato is a world-wide important mining district, particularly for silver production, the geology and stratigraphy of the Guanajuato caldera's portion and vicinity have been studied since many decades ago (e.g., Wandke & Martínez, 1928; Edwards, 1955; Echegoyén-Sánchez *et al.* 1970). Integrating these pioneer studies with the more recent ones of the 90s and 2000s, mentioned previously, the principal Cenozoic stratigraphic packages, from base to top are: (1) the Guanajuato Red Conglomerate, a 1,500–2,000 m thick sequence of continental fluvial deposits; (2) the Loseros-Bufa-Calderones pyroclastic succession, including thinly laminated PDC deposits and thick massive ignimbrites; and (3) a series of dacitic to rhyolitic domes represented by El Rodeo domes, the Peregrina dome and the Chichíndaro dome, and (4) the Cedro Andesite, which consists of mafic to intermediate lava flows apparently fed from fissures, now exposed as dikes in the area.

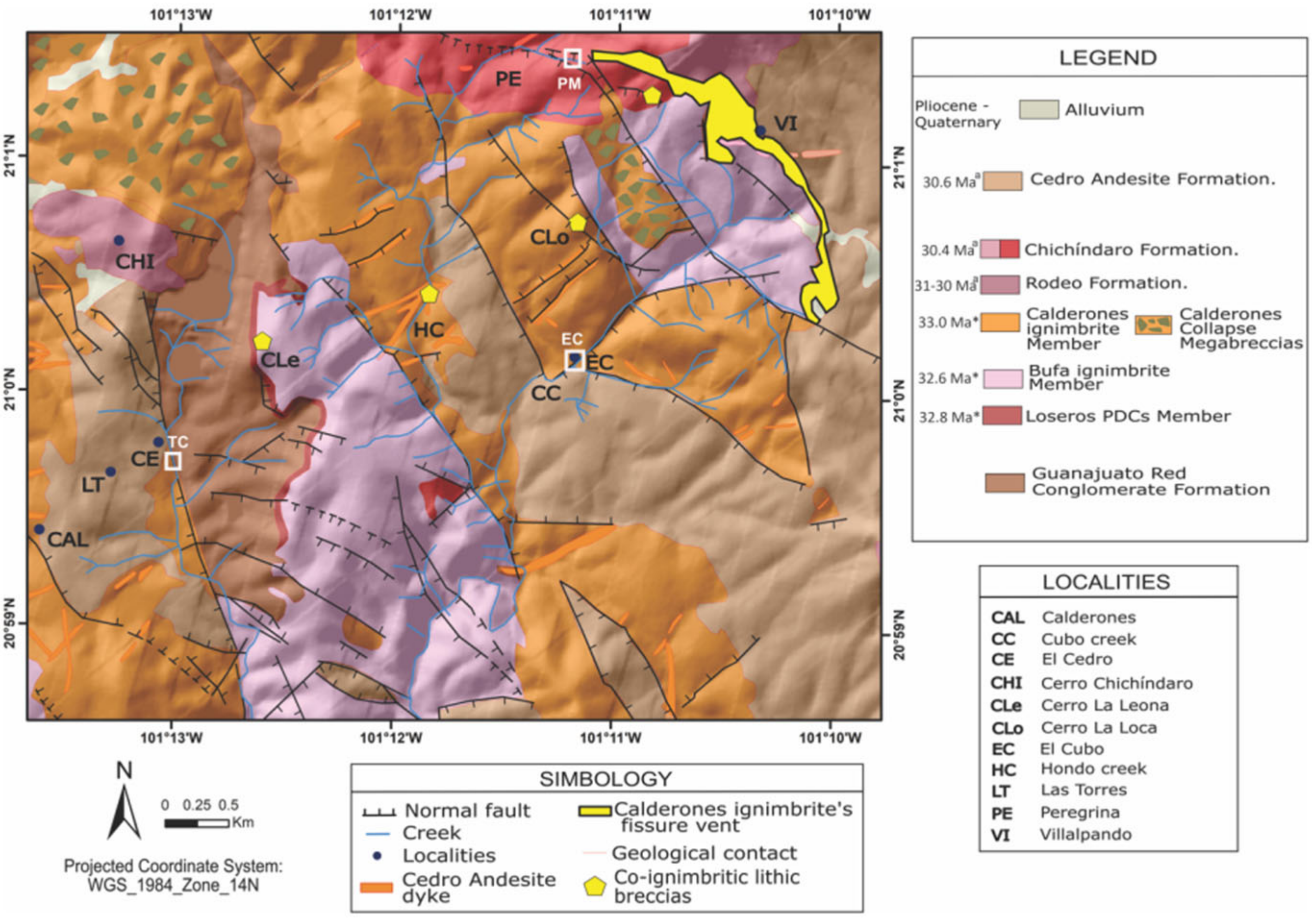

Figure 4. Geologic map of the central-eastern part of the Guanajuato graben caldera and the Guanajuato Mining District (Torres-Peregrina-El Cubo-Peregrina mines) showing intra-caldera normal faults.

Figure 5. Panoramic view of the ESE caldera border (skyline), intra-caldera sector and part of the Guanajuato Mining District (front), including Peregrina and El Cubo mines, and geologic features of Cerro La Loca, and Cerro de Villalpando. Photographs taken from top of Cerro La Leona. The dashed line marks the intra-caldera wall border, behind which is the Sierra Vein System.

Figure 3 shows the geologic map of the Guanajuato caldera and the periphery, and Figure 4 indicates, with more detail, the intra-caldera geology of the eastern portion of the Guanajuato Mining District. A general view of the central part of the caldera and the ESE caldera border is shown in Figure 5, where the trace of the topographic caldera wall is marked by the rim lava domes of the El Rodeo Formation.

Following the recommendation of Martí *et al.* (2018) for the volcanic stratigraphy of a volcanic edifice or system, we redefine the stratigraphy of the Guanajuato Caldera System as follows, the Guanajuato Pyroclastic Formation that consists of a pyroclastic series composed of three members; from base top, Loseros PDC deposits, Bufa Ignimbrite and Calderones Ignimbrite; the El Rodeo Formation that refers to the caldera margin felsic domes; and the Chichíndaro Formation defined here as the group of intra-caldera felsic lava domes that includes the Chichíndaro and the Peregrina members. The Cedro Andesite Formation, composed of mafic lava flows and mafic feeder mafic dikes, is uncertain about its relationship with the Guanajuato caldera system, as explained below. The use of Formation for a sequence, or a unit, is based on that the sequence (or unit) is limited by major unconformities (Martí *et al.* 2018), and this sequence or unit must be described litho-stratigraphically with a type locality and a with a defined distribution to be observed in a map (International Commission

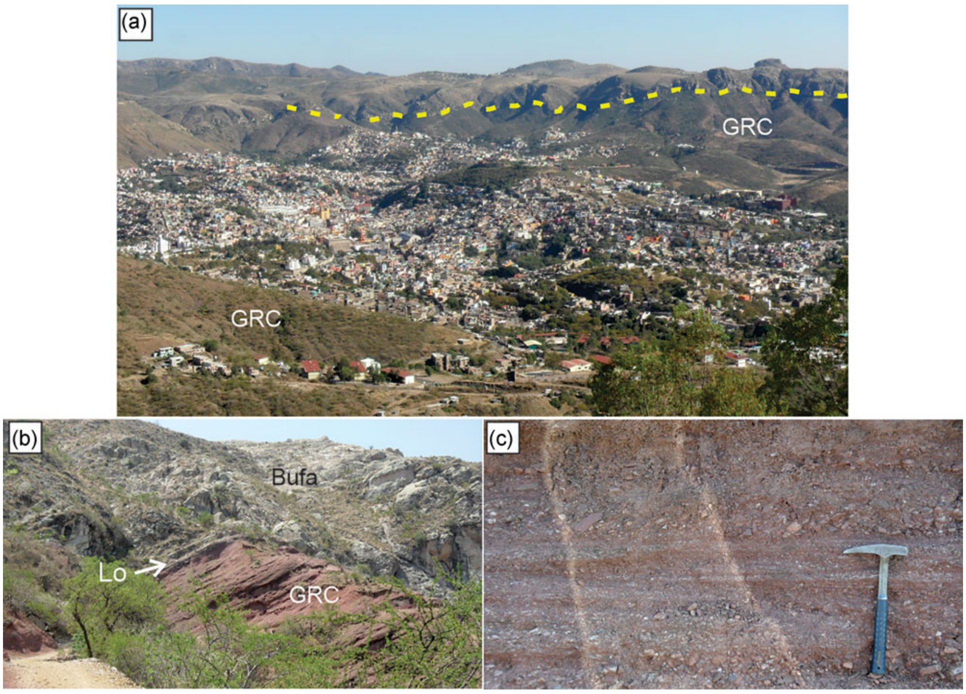

Figure 6. Images of the Guanajuato Red Conglomerate Formation (GRC). (a) Panoramic view of the City of Guanajuato, which is sited mostly on the Red Conglomerate Formation (reddish ground), dashed yellow line is the approximate contact between the conglomerate and upper volcanic units. (b) View of the contact between the conglomerate (red stratified unit) and the upper volcanic units of Loseros (Lo, at the contact with the conglomerate) and Bufa Ignimbrite (massive white rock) overlying Loseros unit. The sequence is tilted to the south, and it can be noticed the concordance along the contact of the conglomerate and Loseros (a photograph of this contact is shown in Fig. 7). (c) Detail of the upper part of the Guanajuato Red Conglomerate at the site shown in b); at this upper part, the unit is mostly gravels and sands with low angle cross-bedding.

on Stratigraphy, 2013); for instance, the Guanajuato Pyroclastic Formation which is composed of three members with concordant contacts between them, and is limited by major unconformities, as described below. We redefine the Guanajuato Volcanic Group proposed by Nieto-Samaniego *et al.* (2016) for the Guanajuato Caldera Volcanic Group that includes all the units related to the Guanajuato caldera system, either pyroclastic deposits or lavas; thus, the group as defined here is formed by the Guanajuato Pyroclastic Formation, El Rodeo Formation and Chichíndaro Formation. Cedro Andesite Formation may be included or not, as it is uncertain its age and its magmatic link to the caldera system.

4.b. Guanajuato Red Conglomerate Formation

The Guanajuato Red Conglomerate Formation was defined by Wandke and Martínez (1928) and was studied thoroughly by Edwards (1955), who mentions a thickness of at least 1,500 m, but Randall *et al.* (1994) assigned 2,000 m to it, which is confirmed by Puy-Alquiza *et al.* (2017). This is a notable thickness considering the relatively small area where this unit crops out, that is, in Guanajuato City and its surroundings (Figs. 3 and 4). It has been reported as an Eocene sequence (Edwards, 1955), and there is a single K-Ar age of 49 Ma obtained from deeply altered (propylitized and chloritized) andesites, apparently interbedded with the conglomerate (Aranda-Gómez & McDowell, 1997), although our observations of the contact relationships of these andesites with the Guanajuato Red Conglomerate are either fault-contact or intrusive-contact. This age should be revised due to the intense alteration of the andesitic lava that may have resulted in the mobilization of the original K content. A single fossil of vertebrate fauna was reported by Ferrusquía-Villafranca (1987) also suggesting an Eocene age, but the wide time-lapse that represents this fossil makes the timing for deposition of this very thick unit less accurate. Thus, the age of the Guanajuato Red Conglomerate is still not well constrained, and its deposition could range in order of several million years, as was described for the nearby Xoconostle Conglomerate, exposed in the adjacent Dolores valley, another basin which continental clastic sediments deposition ranges from Oligocene to Pleistocene (Cerca-Martínez *et al.* 2000). The Guanajuato Red Conglomerate unconformably overlies Mesozoic rocks that compose the regional basement of the area (Edwards, 1955; Martínez-Reyes, 1992; Randall *et al.* 1994). It is generally in fault contact with the basement rocks, as in the ENE Aldana and the Veta Madre faults (Figs. 3 and 4). The Guanajuato Red Conglomerate is a highly indurated continental sedimentary rock with various colours depending on its alteration state, brown, red, grey, green or purple, although reddish-brown is the most common (Fig. 6). Granulometry ranges from sands to conglomerates, with diverse clasts and clast-sizes of granite, gabbro, tonalite, schist, limestone, shales, andesite and dacite, cemented by calcite, silica and limonite, giving the conglomerate a strong concrete-like appearance. The conglomerate was formed by the accumulation of alluvial-fan deposits that developed an intercalated cross-bedded succession within a tectonic-developed depocentre. The clasts are generally subangular and with sand to block boulder sizes (<40 cm). The upper contact with Loseros unit is concordant at the localities that we have examined (Fig. 7; see below the Loseros PDC deposits Member's description), although previous authors indicate an erosional unconformity between these two units (e.g., Echegoyén-Sánchez *et al.* 1970; Randall *et al.* 1994; Nieto-Samaniego *et al.* 2016).

4.c. Loseros PDC Deposits (PDCD) Member

Overlying the Guanajuato Red Conglomerate is the Loseros unit (Fig. 7), which was described originally as a sandstone by Guiza *et al.* (1949), and in more recent works, its sedimentary subaqueous origin is still favoured (Puy-Alquiza *et al.* 2014). Our observations indicate that it is a thinly layered series of dilute PDC deposits, (PDCD), red or pale pink at the contact with the Guanajuato Red Conglomerate and

https://doi.org/10.1017/S0016756825100071 Published online by Cambridge University Press

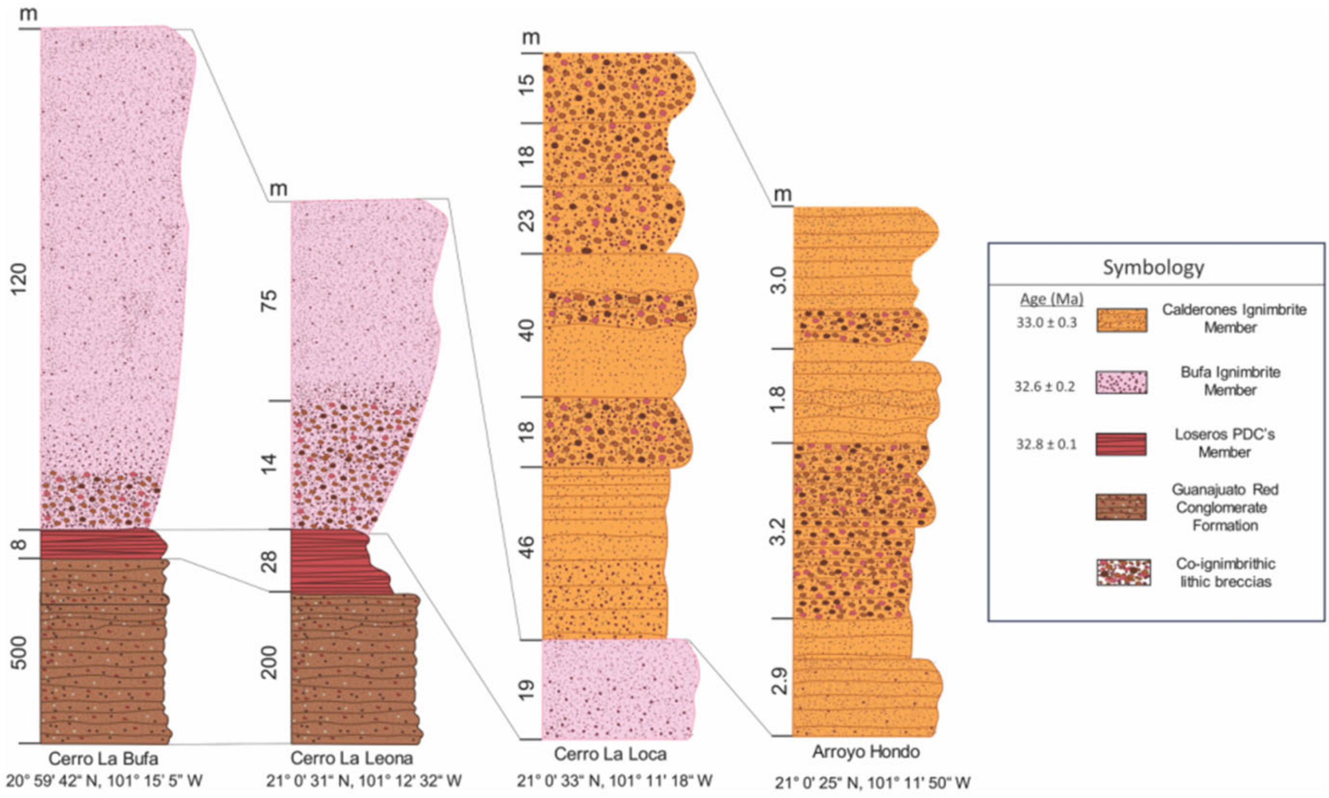

Figure 7. Stratigraphic sections at the type localities and correlation of the Guanajuato Pyroclastic Formation. The Guanajuato Red Conglomerate is shown for reference in some sections. U-Pb ages reported in this work (Table 2) are indicated in the symbology. Thickness of units in m.

green from about the lower-half zone to the top (Fig. 8a, b). It is also in concordant contact with the upper unit, Bufa Ignimbrite (Fig. 8d). Loseros unit is devitrified and chloritized, resulting in its characteristic green colour, except its base, which is generally oxidized and thus, pink to red. It is a thinly layered sequence with low-angle cross-bedding (Fig. 8c), composed of fine to medium ash, including sparse broken angular phenocrysts of sanidine and quartz and accessory zircon, subangular and elongated pumice fragments, subangular lithic clasts and a glass-shards matrix (Fig. 8e, f). The lithics content is poor and occasionally there are lithics larger than 2 cm of hydrothermally altered lava. Rare ripple-marks-like structures in sparse sites have been reported that are probably due to seismicity on soft and humid PDC fine ash deposits (Alquiza & Avilés, 2015), seismicity that we interpret as a result of the caldera volcanic activity and collapse. Our observations indicate that the first PDCD of Loseros were apparently deposited in thin water tables or shallow ponds developed on the top of the Guanajuato Red Conglomerate, whereas later-arriving PDCs were subaerial deposits above the water tables levels. The thickness of Loseros unit varies from 0.0 to 22 m (Figs. 2 and 7). The outcrops occur just beneath the next unit, the Bufa Ignimbrite (Figs. 8d and 9d). At several localities, the contact between Loseros and Bufa is concordant, although Bufa's dense PDCs eroded the top of Loseros unit at some sites. The type locality of Loseros unit is the same as Bufa Ignimbrite at the site known as La Cueva at the base of Cerro La Bufa (Fig. 7), just to the south of Guanajuato City (Fig. 3). The U-Pb age of Loseros PDCD reported by Coutiño-Taboada (2015) and Aguirre-Díaz *et al.* (2016) yielded about 32.5 Ma (Table 1), but an actualized age resulted in 32.8, using a newer data reduction software, is presented in Section 5 and Table 2). Loseros unit is redefined here as the Loseros PDCD Member of the Guanajuato Pyroclastic Formation since there is no unconformity between Loseros PDCD and the Bufa Ignimbrite and forms part of the volcanic system of the Guanajuato caldera.

4.d. Bufa Ignimbrite Member

Concordantly overlying Loseros PDCD is the Bufa Ignimbrite, originally defined as Bufa Rhyolite Formation by Wandke and Martínez (1928), who interpreted it as rhyolitic tuffs and lavas. It is a massive light pink to light grey ignimbrite with about 5 vol.% of crystal content including sanidine, quartz and sparse plagioclase and biotite (Fig. 9). The type locality is at Cerro La Bufa (Fig. 7). In general, it is a devitrified deposit with vapour-phase silica induration at the top; it is partly welded and with columnar jointing (Fig. 9). Our records indicate that the ignimbrite has a maximum thickness of 300 m (Fig. 2), but it can reach 360 m according to Randall *et al.* (1994), or 400 m as reported in Nieto-Samaniego *et al.* (2016). Lithics of several lithologies are concentrated at the base, just above the contact with the Loseros PDCD Member (Figs. 8d and 9d). It is concordantly overlaid by the Calderones PDC deposits. Pumice lumps were mostly destroyed by devitrification and silicification, but they can still be recognized. In other cases, the pumices are inferred from the moulds left after erosion. Using these moulds, pumice sizes reach up to 35 cm. Co-ignimbrite lithic lag breccias are relatively common at the base of Bufa Ignimbrite (Fig. 9b) and generally occur next to major normal faults that bound the Guanajuato caldera and next to intra-caldera normal faults (Figs. 3 and 4). These breccias are heterolithologic and include clasts of granite, tonalite, schist, intermediate composition lavas, welded ignimbrites, and of the Guanajuato

https://doi.org/10.1017/S0016756825100071 Published online by Cambridge University Press

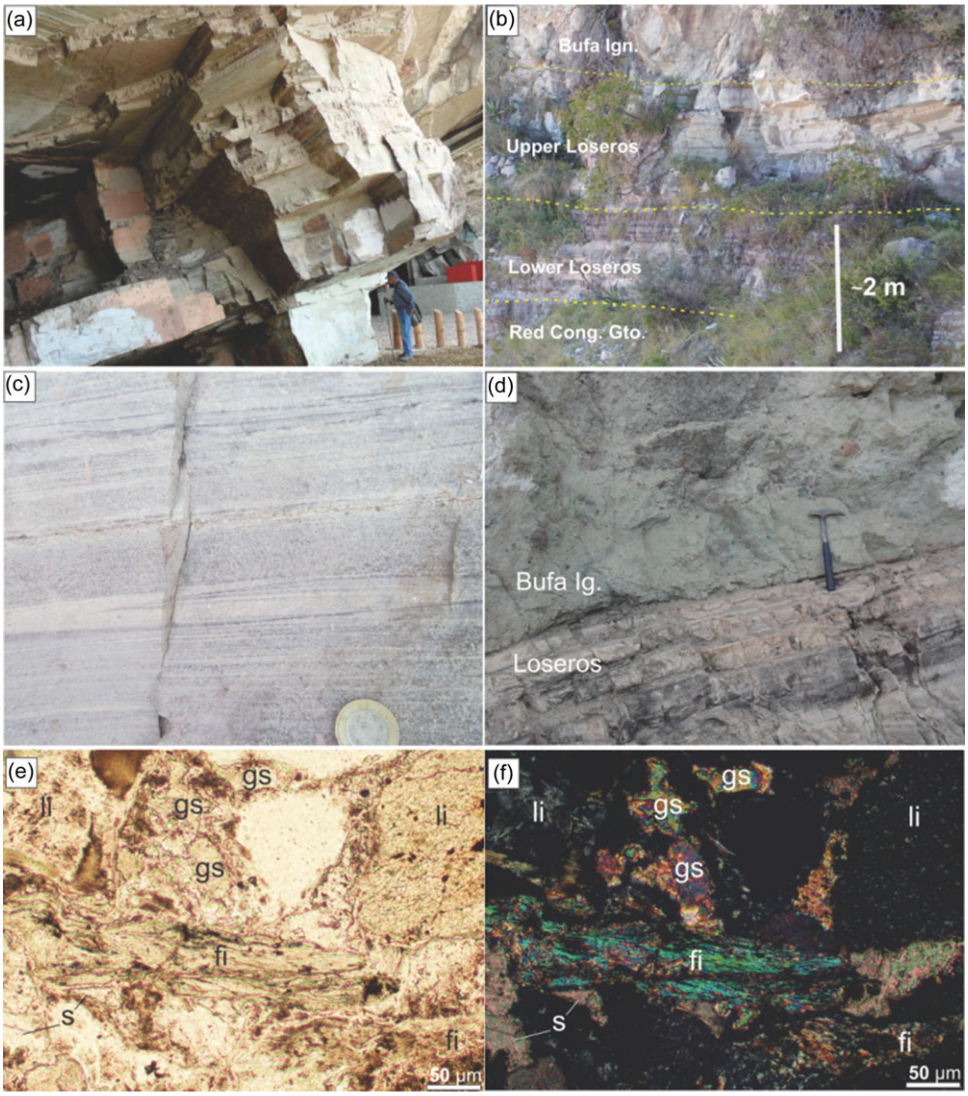

Figure 8. Images of the Loseros PDCD Member. (a) General view of the type locality in La Cueva (The Cave), at Cerro La Bufa, showing the Loseros PDC deposits, thinly stratified, and in contact with La Bufa Ignimbrite (roof of cave); (b) Concordant contact between the top of the Guanajuato Red Conglomerate and the Loseros unit exposed at the base of Cerro La Bufa; (c) detail of the aspect of the Loseros unit showing low-angle cross-bedding and thin layering, which indicate high-energy fluidization dynamics common in PCD dilute deposits; (d) detail of the upper, sharp, concordant, contact of Loseros PDC deposits with Bufa Ignimbrite, showing a continuous deposition between the two units; note lithics concentration base zone of Bufa Ignimbrite and green colour due to chloritization. (e) and (f) photomicrographs of the Loseros unit showing the pyroclastic nature of the deposit, with chloritized, collapsed, pumice fragments (fiamme-fi), quartz (q), sanidine (s), and angular lithic clasts (li), within a chloritized, glass-shards (gs) ash matrix; (e) parallel light image, and (f) polarized light image.

Red Conglomerate. Clasts in the co-ignimbrite lag breccias are angular to subrounded, and with sizes up to 33 cm. The Bufa Rhyolite is here redefined as the Bufa Ignimbrite Member of the Guanajuato Pyroclastic Formation, as there are no unconformities with the lower and upper pyroclastic units, that is, Loseros PDCD and Calderones Ignimbrite, respectively, and Bufa Ignimbrite forms part of the Guanajuato caldera volcanic system. The age of Bufa Ignimbrite reported by Coutiño-Taboada (2015) and Aguirre-Díaz *et al.* (2016) is within 32 to 33 Ma (Table 1), but an actualized age resulted in 32.6 Ma, using a newer data reduction software, and presented in Section 5 and Table 2. Nieto-Samaniego *et al.* (2016) report an age of 33.5 Ma (Table 1).

4.e. Calderones Ignimbrite Member

The Calderones Formation was originally defined by Echegoyén-Sánchez *et al.* (1970) as continental clastic deposits, referring to conglomeratic deposits, with its type locality at Calderones village, just to the southeast of Guanajuato City (Figs. 3 and 4). This sequence is redefined here as the Calderones Ignimbrite Member of the Guanajuato Pyroclastic Formation, as it conformably overlies the Bufa Ignimbrite Member (Fig. 7) and forms part of the Guanajuato caldera volcanic system. Although its formal name comes from Calderones village area, the best sequence was observed at Cerro La Loca (Fig. 7), near El Cubo mine (Figs. 3 and 4), which may better represent the type locality, but we have decided to keep the original name of Calderones to avoid new names for the units that may create confusion. Calderones Ignimbrite was dated within 32.5 and 33.2 Ma (Coutiño-Taboada, 2015; Aguirre-Díaz *et al.* 2016; Table 1) An actualized age resulted in 33.0 Ma, and details are mentioned in Section 5. Nieto-Samaniego *et al.* (2016) dated it at 31.8 to 31.3 Ma.

Calderones Ignimbrite is a stratified succession of PDC deposits, ranging from dilute PDCs that form thin, cross-bedded deposits (Fig. 10b), to dense PDCs that form massive and thick ignimbrites (Fig. 10a), these last ones particularly at the top of the sequence (Fig. 7). The layered sequence generally consists of green, lithics-rich to lithics-poor deposits, supported by a chloritized matrix made of fine to coarse ash (Fig. 10e, f). The layered characteristic and the lithics-rich nature of the deposits were probably the cause of originally misinterpreting it as a conglomerate. However, since 1993, several authors describe it as pyroclastic rocks (Aranda-Gómez *et al.* 2003; Randall *et al.* 1994; Aguirre-Díaz *et al.* 2012*a*, 2012*b*, 2014; Coutiño-Taboada, 2015; Nieto-Samaniego *et al.* 2016). The contact between Bufa

https://doi.org/10.1017/S0016756825100071 Published online by Cambridge University Press

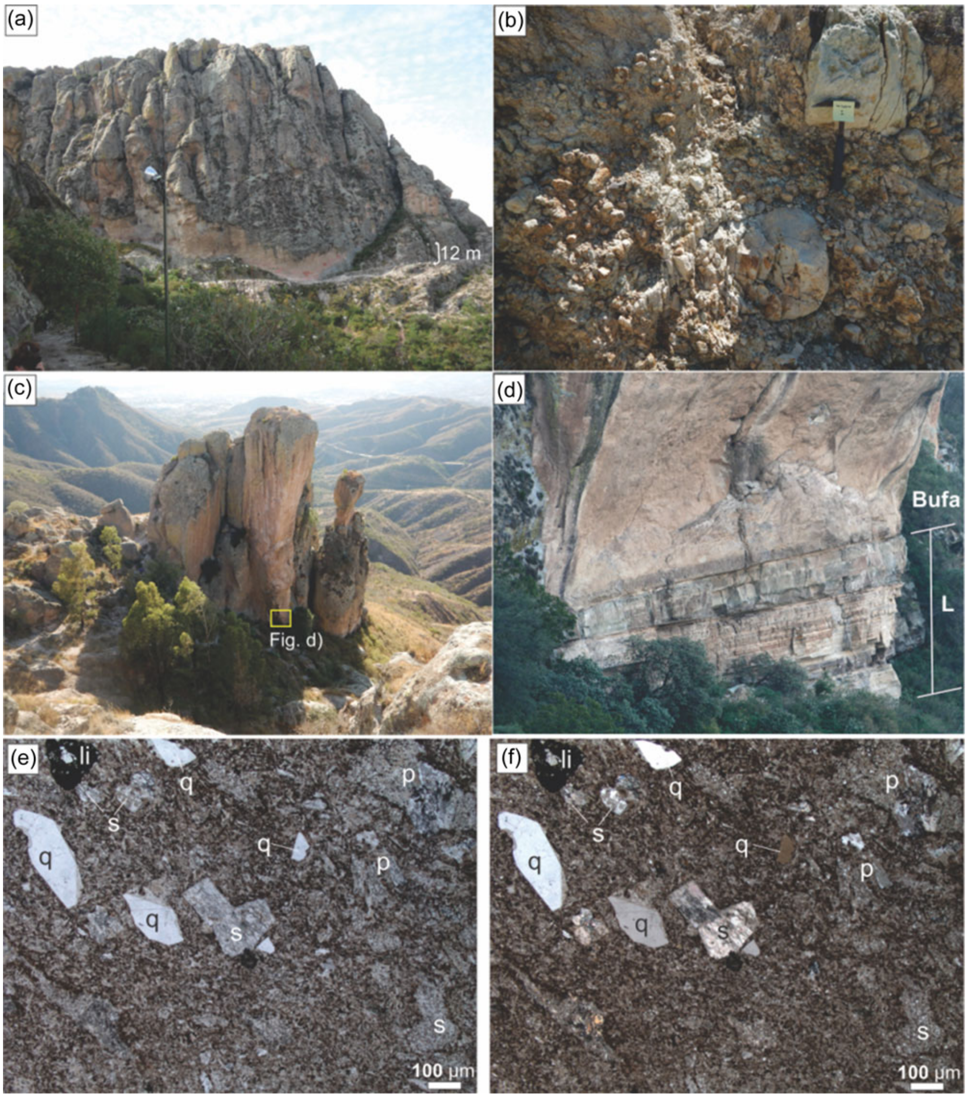

Figure 9. Images of the Bufa Ignimbrite. (a) General view of the type locality at Cerro La Bufa (note scale in m); (b) Co-ignimbrite lithic breccia at the basal zone of Bufa Ignimbrite at Cerro La Leona site; lithics are mostly of rhyolitic lava, but there are also altered andesitic lavas and sparse clasts from local Mesozoic basement; (c) Panoramic view of Bufa Ignimbrite eroded columns to the south of Cerro La Bufa; the rectangle drawn at the base of the ignimbrite marks the site of next image; (d) Detail of sharp contact of Bufa Ignimbrite with Loseros unit. (e) and (f) photomicrographs of Bufa Ignimbrite, parrallel light and polarized light, respectively, showing a pyroclastic partly welded texture mostly composed of devitrified glass shards with phenocrysts of quartz (q), plagioclase (p) and sanidine (s), as sparse lithic clasts.

Ignimbrite and Calderones Ignimbrite is concordant, generally parallel and without evidence of deposition interruption, such as paleosols or fluvio-lacustrine deposits, but, in some cases, Calderones' initial PDCs eroded the top of the Bufa Ignimbrite, forming a channelized contact. In general, green, small pumice, or green small fiamme when welded, can be observed throughout the sequence. Calderones Ignimbrite includes three subunits, the Lower, Middle and Upper zones (Fig. 7). The Lower zone is a thinly layered series, 10–50 cm thick, lithics-rich and with low-angle cross-bedding, made from a continuous accumulation of dilute PDCs (Fig. 10b). The Middle zone is made of denser PDC deposits that form thicker (1–3 m) ignimbrites. The Upper zone consists of a series of three thick, massive ignimbrites, 5 to 10 m thick each (Fig. 10a). These upper ignimbrites include co-ignimbrite lithic lag breccias at some places, particularly at Cerro La Loca (Fig. 10c) and at Cerro de San Nicolás localities (Figs. 3 and 4), with basement lithics carried up from the conduit including tonalite, granite, diorite, schist, phyllite, andesite, dacite and Red Conglomerate of Guanajuato. A notable case is the megabreccia observed at the base of Cerro de Villalpando, with mega-blocks reaching sizes of 3–6 m, including basement rocks (schist or phyllite of Esperanza Formation) and of Guanajuato Red Conglomerate, all within a green-brown pumiceous matrix of the Calderones Ignimbrite (Fig. 10c). The composition of Calderones Ignimbrite is intermediate, apparently andesitic-dacitic based on the mineralogy, consisting of plagioclase, pyroxene and hornblende. The rock is too altered for obtaining a secure TAS classification via major elements chemistry. The whole sequence is pervasively chloritized.

4.f. El Rodeo Formation-caldera margin domes

The Guanajuato Mining District area is bounded by a chain of felsic lava domes that include the El Rodeo rhyolite in the southwestern part of the district, and felsic domes that extend along the Sierra Vein System at the eastern portion of the district from El Rodeo to Santa Rosa towns (Figs. 3, 5 and 11a). This unit is redefined here as El Rodeo Formation, as it is stratigraphically bound by unconformities representing a volcanic quiescence after Calderones Ignimbrite´s emplacement. The domes vary in composition from dacitic to rhyolitic based on their mineralogy; felsic domes contain phenocrysts of sanidine, quartz, accessory apatite and, occasionally, biotite in the rhyolitic ones, and plagioclase and orthopyroxene in the dacitic ones (Fig. 11c, d). The main characteristics are those commonly observed in felsic

https://doi.org/10.1017/S0016756825100071 Published online by Cambridge University Press

Table 1. Ages reported by other authors and this work of the Guanajuato caldera products

Unit	Method	Age (Ma) ± 1 σ	Reference
Cedro Andesite	K-Ar	30.6 ± 0.4	Cerca-Martínez *et al.* 2000
	K-Ar	30.7 ± 0.6	Cerca-Martínez *et al.* 2000
	U-Pb zircon	32.53 ± 0.18	Nieto-Samaniego *et al.* 2016
	U-Pb zircon	32.58 ± 0.21	Nieto-Samaniego *et al.* 2016
Chichíndaro Rhyolite	K-Ar	32 ± 1	Gross, 1975
	K-Ar	30.1 ± 0.8 (Santa Rosa)	Nieto-Samaniego *et al.* 1996
	K-Ar	30.8 ± 0.8 (El Rodeo)	Nieto-Samaniego *et al.* 1996
	U-Pb zircon	30.36 ± 0.4	Nieto-Samaniego *et al.* 2016
Calderones Ignimbrite	U-Pb zircon	32.54 ± 0.56	Aguirre-Díaz *et al.* 2016
	U-Pb zircon	33.22 ± 0.46	Aguirre-Díaz *et al.* 2016
	40Ar-39Ar	31.33 ± 0.29	Nieto-Samaniego *et al.* 2016
	U-Pb zircon	31.84 ± 0.27	Nieto-Samaniego *et al.* 2016
Bufa Ignimbrite	U-Pb zircon	33.57 ± 0.22	Aguirre-Díaz *et al.* 2016
	U-Pb zircon	33 ± 0.3	Aguirre-Díaz *et al.* 2016
	40Ar-39Ar	33.53 ± 0.48	Nieto-Samaniego *et al.* 2016
Loseros PDCP	U-Pb zircon	31.96 ± 0.27	Aguirre-Díaz *et al.* 2016
	U-Pb zircon	33.00 ± 0.28	Aguirre-Díaz *et al.* 2016

domes, such as concentric dome foliation flow-banding and auto brecciated lavas in the external facies of the domes. Devitrification, silicification and oxidation are common in these lavas, with hydrothermally altered zones (Fig. 11b). These lavas overlie or intrude Bufa and Calderones members and are here interpreted as post-collapse domes that were emplaced along the caldera marginal faults marking the Guanajuato caldera's border (Figs. 3–5). The age of this unit is about 31 to 30 Ma, considering the K-Ar ages reported by Nieto-Samaniego *et al.* (1996) that they named as Chichíndaro Rhyolite, in samples collected near Santa Rosa in the north, and near El Rodeo in the south (30.1 ± 0.8 Ma and 30.8 ± 0.8 Ma, respectively; Table 1).

4.g. Chichíndaro Formation-intra-caldera domes

This unit is interpreted here as the felsic lava domes that were emplaced inside the Guanajuato caldera, that is, intra-caldera domes; it includes the Chichíndaro Rhyolite Member and the Peregrina Dacite Member. Both domes formed after the collapse of the caldera, and unconformably overly units of the Guanajuato Pyroclastic Formation.

4.g.1. Chichíndaro Rhyolite Member

Chichíndaro Rhyolite was originally defined by Wandke and Martínez (1928) as rhyolitic lavas with the type locality at Cerro Chichíndaro (Fig. 3). Cerro Chichíndaro is a small and elongated rhyolitic dome in the central portion of the caldera that apparently used a major normal fault as conduit, the Veta Madre fault, since the dome overlies the fault, but it is not displaced by it (Figs. 12a and 13a). Small rhyolitic domes of Chichíndaro Rhyolite crop out scattered throughout the mining district that are too small to be shown in the geologic map (Figs. 3 and 4) but are marked in the detailed geologic maps of Echegoyén-Sánchez *et al.* (1970). Chichíndaro Rhyolite unconformably overlies either the Guanajuato Red Conglomerate Formation, Calderones or Bufa ignimbrite members. These lava domes are crystal-poor, flow-banded, devitrified, and silicified rocks, with lava dome concentric foliation and some, as Cerro Chichíndaro, with lens-shaped structures on map view. Quartz and sanidine are the main minerals with sparse oxidized biotite making all about 3–5 vol. % (Fig. 12c, d). Some domes, such as Cerro Chichíndaro, were preceded with explosive eruptions that formed pyroclastic fan deposits adjacent to the dome. Chichíndaro Rhyolite has been dated at 32 ± 1 Ma (K-Ar age; Gross, 1975) and at 30.36 ± 0.4 Ma (Ar-Ar age; Nieto-Samaniego *et al.* 2016; Table 1); the more precise age of 30.4 ± 0.4 Ma is apparently the best age.

4.g.2. Peregrina Dacite Member

Echegoyén-Sánchez *et al.* (1970) define this unit as the Peregrina Intrusive, given the intrusive contact observed in outcrops and in tunnels of the local mines. However, in this work, and in previous reports (Randall *et al.* 1994; Aguirre-Díaz *et al.* 2012*a*, 2012*b*, 2014), this intrusive is interpreted as a volcanic dome (Figs. 12e, f and 13b) with intrusive contacts in some sites and lava flow contacts in other sites. The Peregrina dome intersects or overlies the Guanajuato Red Conglomerate, the ignimbrites of the Guanajuato Pyroclastic Formation and lavas of the Chichíndaro Rhyolite Formation; this last observation according to Echegoyén-Sánchez *et al.* (1970). Peregrina's lavas contain plagioclase, sanidine and quartz phenocrysts that make about 5–10 vol.% of the rock, within a devitrified matrix. Dome flow foliation is characteristic, and lava autobreccias of the external zone of the dome are observed at its southwestern flank (Fig. 12f). In general, the lavas are intensively hydrothermally altered, including oxidation, propylitization and silicification. There are no public reports of an isotopic age of this unit but stratigraphically it is younger than, or contemporaneous with, Chichíndaro Rhyolite Member.

4.h. Cedro Andesite Formation

The Cedro Andesite Formation was defined by Echegoyén-Sánchez *et al.* (1970). This unit consists of mafic lava flows, generally brown or dark grey in sparse fresh rock outcrops. Lavas are highly altered and weathered, and apparently, some lavas were deposited underwater. Cedro Andesite occurs as scattered lavas throughout the Guanajuato Mining District and unconformably overly the Guanajuato Red Conglomerate and Bufa and Calderones ignimbrites. Exposures of this andesite are also observed outside the caldera margin to the east (Cerca-Martínez *et al.* 2000; Nieto-Samaniego *et al.* 2016). Lavas are porphyritic but fine-grained, with phenocrysts of plagioclase and pyroxene; the matrix is commonly highly weathered and altered but in freshest samples, patches of microcrystalline texture can be observed with

https://doi.org/10.1017/S0016756825100071 Published online by Cambridge University Press

Table 2. U-Pb zircon ages of the Guanajuato Pyroclastic Formation reported in this work

Unit	Sample	Location	Coordinates UTM 14Q Latitude N	Coordinates UTM 14Q Longitude E	Elevation (m)	Method	Age Ma ± 1 σ	Average age Ma ± 1 σ
Calderones Ignimbrite	GUA-41	Road Guanajuato- Santa Rosa	2331285	269894	2622	U-Pb zircon	32.86 ± 0.37	33.0 ± 0.3
	GUA-28	Hondo Creek (road to El Cubo)	2324302	271622	2228	U-Pb zircon	33.16 ± 0.18	
Bufa Ignimbrite	GUA-23	Road from Olla dam to Calderones	2324091	268399	2226	U-Pb zircon	33.85 ± 0.12	32.6 ± 0.2
	GUA-20	La Cueva at Cerro La Bufa	2322950	265894	2235	U-Pb zircon	31.31 ± 0.22	
Loseros PDCP	GUA-19	La Cueva at Cerro La Bufa	2323043	265984	2230	U-Pb zircon	31.95 ± 0.08	32.8 ± 0.1
	GUA-32	Cerro La Leona	2324495	270405	2500	U-Pb zircon	33.53 ± 0.19	

U-Pb analyses performed with ICP-MS-LA at the Isotopic Studies Laboratory of Geosciences Institute, UNAM.
Age results on the basis of 35 zircon analyses per sample, with a mean value at 95% confidence.
Coordinates are UTM, Zone 14Q, Datum Nad27; elevation in meters above sea level.

plagioclase microlites. These lavas may be correlated with several mafic dikes that crosscut the Guanajuato Pyroclastic Formation throughout the interior of the caldera that were mapped in detail by Echegoyén-Sánchez *et al.* (1970), referring to them as Porphyry Andesite and Diabase. Particularly, good outcrops of the dikes occur near Calderones village, cutting the Calderones Ignimbrite Member and along Hondo creek (Fig. 4). Mafic dikes are generally oriented ENE-WSW, and range in width from less than 1 m to about 6 m. Texturally, they are fine-grained dark grey lavas when fresh, with sparse phenocrysts of plagioclase and pyroxene. We interpret them as feeder dikes for the Cedro Andesite lavas, as both have similar textural aspects and stratigraphically are younger than Calderones and Bufa ignimbrites. Andesitic lavas exposed outside the Guanajuato caldera and within the Sauceda Graben that have been correlated with Cedro Andesite were dated with K-Ar technique at 30.6 ± 0.4 Ma and 30.7 ± 0.6 Ma, in two separate samples by Cerca-Martínez *et al.* (2000; Table 1). Nieto-Samaniego *et al.* (2016) dated them at 32.6 to 32.5 Ma with the U-Pb zircon method, including a dike. Thus, Cedros Andesite's age may be about 32.5 Ma or about 30 Ma, depending on the method used. We did not find a clear contact of this unit with Chichíndaro Formation. Any of these timings could fit well with the geologic record, but for now, we prefer the age of 30.6–30.7 Ma obtained by the K-Ar method (Cerca-Martínez *et al.* 2000), which agrees with the preference of Nieto-Samaniego *et al.* (2016).

5. U-Pb age results of the Guanajuato Pyroclastic Formation reported in this work

We obtained 6 zircon U-Pb ages of the Guanajuato Pyroclastic Formation members including Loseros PDCD, Bufa Ignimbrite and Calderones Ignimbrite. The data were first reported in the thesis of Coutiño-Taboada (2015) and were mentioned in an abstract in Aguirre-Díaz *et al.* (2016). Here, we present the actualized U-Pb data (Table 2, Fig. 14a–c) using the data processing tool of IsoplotR for age calculation (Vermeesch, 2018). Full data have not been published before, and the complete dataset is presented here. Locations of dated samples are shown on the geological map (Fig. 3). Full data analyses can be found in the Supplementary Material.

Rounding the values to 1 decimal point and referring to results shown in Table 2, two ages of Loseros PDCD resulted in 32.0 ± 0.1 Ma for sample GUA-19 collected at La Cueva site (Loseros PDCD-Bufa Ignimbrite type sections; Fig. 7), and 33.5 ± 0.2 Ma for sample GUA-32 collected at the top of Cerro La Leona (section Cerro La Leona, Fig. 7); the average of both results is the representative age of 32.8 ± 0.1 Ma (Table 2). Two samples of Bufa Ignimbrite were dated; the sample GUA-20 collected at La Cueva-Cerro La Bufa (Fig. 7) yielded an age of 31.3 ± 0.2 Ma, whereas the sample GUA-23 collected at a road cut between La Olla dam and Calderones yielded 33.9 ± 0.1 Ma; the average of these two results of 32.6 ± 0.2 Ma is the most representative for this unit (Table 2). Two samples of Calderones Ignimbrite were selected for U-Pb zircon dating; sample GUA-28 collected at Hondo Creek (Fig. 7) yielded 33.2 ± 0.2, and sample GUA-41 collected at the extra-caldera facies of the unit along the highway of Guanajuato-Santa Rosa yielded 32.8 ± 0.4 Ma, with an average age resulting in 33.0 ± 0.3 Ma (Table 2). The average ages of Loseros and Bufa units are similar at around 32.8–32.6 Ma, but Calderones unit results are somewhat older at 33.0 ± 0.3, perhaps because xenocrystals of zircon were difficult to recognize during the hand-picking removal of lithics and xenocrystals in the sample preparation procedure. Geological observations indicate a concordant contact between the three members, Loseros-Bufa-Calderones, and they should have been emplaced continuously, as discussed in Section 7. The average age obtained for the three units of the Guanajuato Pyroclastic Formation is 32.8 ± 0.2 Ma, which represents the approximate time of the caldera collapse and the emplacement of this voluminous formation.

6. Tectonic structure of the Guanajuato caldera

The southern portion of the Sierra de Guanajuato was affected by intense normal faulting during the Cenozoic, with faults following two main orientations, NW-SE and NE-SW, which has been related to the extension of the Basin and Range tectonic province in Mexico (Fig. 1; Stewart, 1978; Henry & Aranda-Gómez, 1992; Aguirre-Díaz & Mcdowell, 1993), and the effect of major crustal block boundaries at surface during extension, apparently during several extensional-transtensional events (Nieto-Samaniego *et al.*

https://doi.org/10.1017/S0016756825100071 Published online by Cambridge University Press

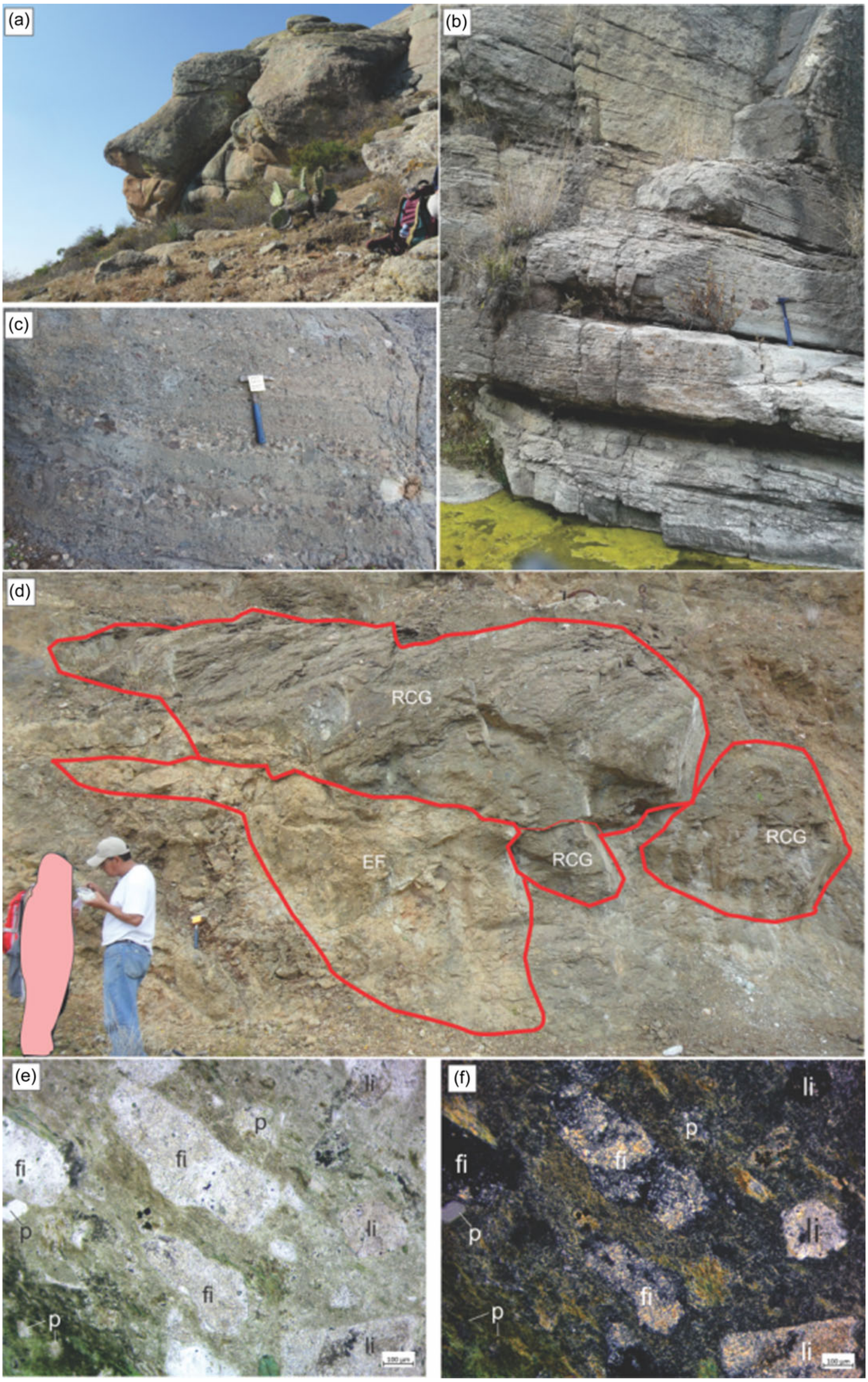

Figure 10. Images of the Calderones Ignimbrite. (a) General view of three uppermost ignimbrites at the top of Cerro La Loca; (b) Lower beds of the Calderones sequence formed by thin to medium thick PDC deposits; (c) Co-ignimbrite lithic breccias at the base of the lower ignimbrite showed in a); (d) Co-ignimbrite megabreccia with blocks that can reach 6 m in length of Red Guanajuato Conglomerate (RCG) and Cretaceous phyllites of Esperanza Formation (EF), which are within a chloritized pumiceous and ash matrix. (e) Photomicrograph of welded ignimbrite showing lithics (li), fiamme (fi) and plagioclase (p), within a welded glass-shard matrix with green tones due to a pervasive chlorite alteration (parallel light): (f) Photomicrograph same as (e) but with polarized light.

2007; Tristán-González *et al.* 2009). Locally, the main faults are El Bajío (NW-SE) which bounds the Sierra de Guanajuato at the southwest, the Villa de Reyes graben (NE-SW) that crosses through the Sierra de Guanajuato, and continues to the north until San Luis Potosí City, the Sauceda graben (NE-SW) that also crosses through this range, but smaller in size than Villa de Reyes, and the local

https://doi.org/10.1017/S0016756825100071 Published online by Cambridge University Press

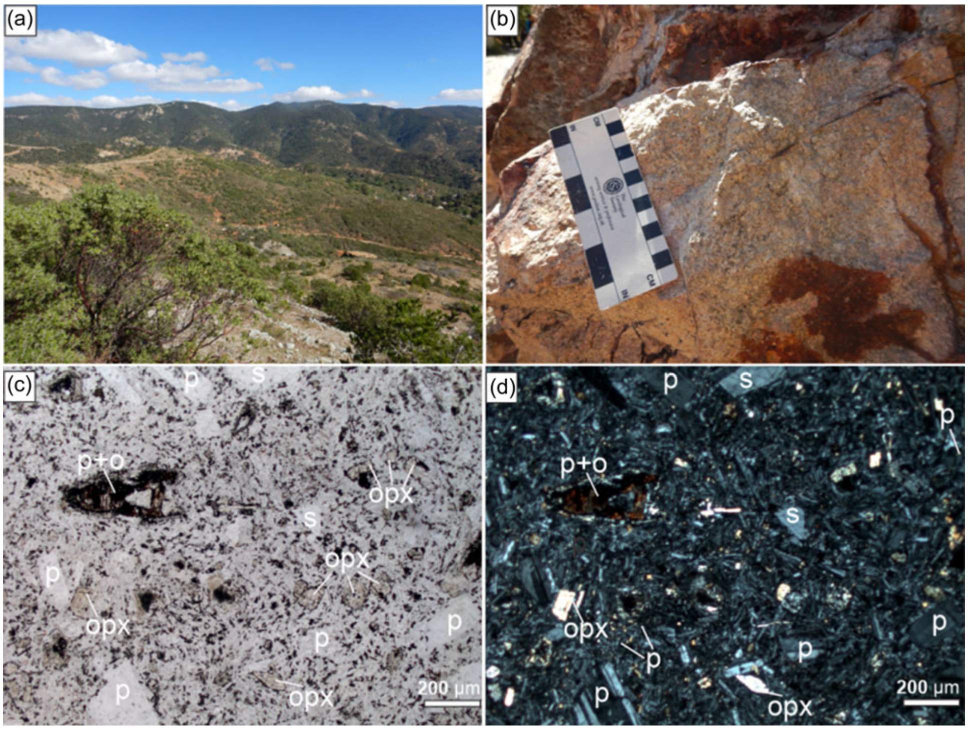

Figure 11. Images of El Rodeo Formation. (a) View of felsic lava domes forming the caldera border (range at skyline). (b) Outcrop of felsic lava with semivertical dome foliation, and slightly oxidized. (c) Photomicrograph with parallel light of felsic lava with a porphyritic, hipocrystalline texture, with phenocrysts of plagioclase (p), sanidine (s), oxides due to alteration (o), and accessory apatite (ap). (d) Same as c but with polarized light.

faults of Veta Madre (NW-SE), the Sierra Veins System (NW-SE) and Aldana (NE-SW) (Figs. 3 and 15). Table 3 includes the structural data of the principal faults in the study area, and location of measuring sites is shown in the geologic and structure maps (Figs. 3 and 15).

These orthogonal faults prepared the tectonic framework within which the graben caldera of Guanajuato was developed (Fig. 16). Before the caldera, the Guanajuato graben was already bordered by NW-SE and NE-SW faults (Figs. 15 and 16). In this tectonic depression, fluvial deposits accumulated in the form of alluvial fans by the erosion of the graben margins resulting in the Guanajuato Red Conglomerate Formation (Fig. 16; Edwards, 1955). The great thickness of 2000 m of this unit suggests a long deposition time during the graben's subsidence. It is uncertain the age for this conglomerate but apparently started at the Eocene and finished at the Oligocene at around 33 Ma. The lower age is based on the fossil age report of Ferrusquía-Villafranca (1987) and the 49 Ma age report of Aranda-Gómez and McDowell (1997), and the upper age is based on the concordant contact with 32.8 Ma Loseros Member reported in this study. The caldera margin faults were tectonically controlled by the orthogonal faults of the pre-existing Guanajuato graben (Figs. 15 and 16); that is, the Aldana fault, that marks the NW margin of the caldera, now exposing a tectonic contact between Mesozoic basement units and the Guanajuato Red Conglomerate Formation; the NW-SE Sierra Veins fault system to the NE together with an inferred fault covered by the domes of El Rodeo Formation (Fig. 15); an inferred NE-SW fault system that forms the SE margin of the caldera buried by the rim lava domes of El Rodeo Formation; and an inferred NW-SE fault to the SW beneath the El Rodeo lava domes that was apparently displaced by the El Bajío fault at this sector, which scarp was later eroded (Fig. 15).

The caldera structure can be visualized in a geologic NE-SW cross-section (Fig. 17), where the broken crust can be noticed within the caldera, represented by several faulted blocks that we interpret as the intra-caldera collapsed blocks, whereas the caldera marginal faults were apparently used as conduits for the magma's ascension to form the post-collapse rim lava domes (El Rodeo Formation). The intra-caldera block faults are several smaller normal faults within the caldera that bound blocks of several sizes (Figs. 4 and 15; Table 3); examples are El Cubo, La Loca, La Leona, Capulín, Calderones, among many others, as shown in the 1:10,000 scale maps of Echegoyén-Sánchez *et al.* (1970), and in Figure 4, which is a representative portion of the intra-caldera faults. These faults and related blocks are here interpreted as the result of the caldera collapse with a piece-meal style; thus, they were produced by gravitational collapse during the formation of the caldera (e.g., Lipman, 1997, Gottsmann and Martí, 2008). Gravitational collapse of intra-caldera blocks can explain the simultaneous displacement of two or more fault surfaces with different strikes, as these fault surfaces correspond to the different fault planes of the subsiding blocks, as has been proposed for the graben-type calderas (Aguirre-Díaz, 2008); for example, the 90 km long Bolaños graben caldera at Jalisco, México (Aguirre-Díaz *et al.* 2021). Within the caldera structure, there is the Veta Madre Fault, oriented NNW-SSE, which crosses through the middle of the caldera area (Figs. 3, 4 and 15). Along this fault, there were emplaced several Ag-Au hydrothermal ore deposits of the Guanajuato Mining District (Randall *et al.* 1994; Orozco-Villaseñor, 2014). This fault apparently continued to be active after the caldera formation and extended beyond the caldera limits to the north.

Tectonic uplifting of the Sierra de Guanajuato as a regional event has been reported in previous works (Nieto-Samaniego *et al.* 2007; Aranda-Gómez *et al.* 2003; Tristán-González *et al.* 2008, 2009), but in a local scale, in particular in the caldera area, uplifting could also be caused by a resurgence final phase of the caldera, modifying the original faults that were formed either by tectonic events or the gravitational collapse of the intra-caldera blocks; the resurgence caldera interpretation is discussed below.

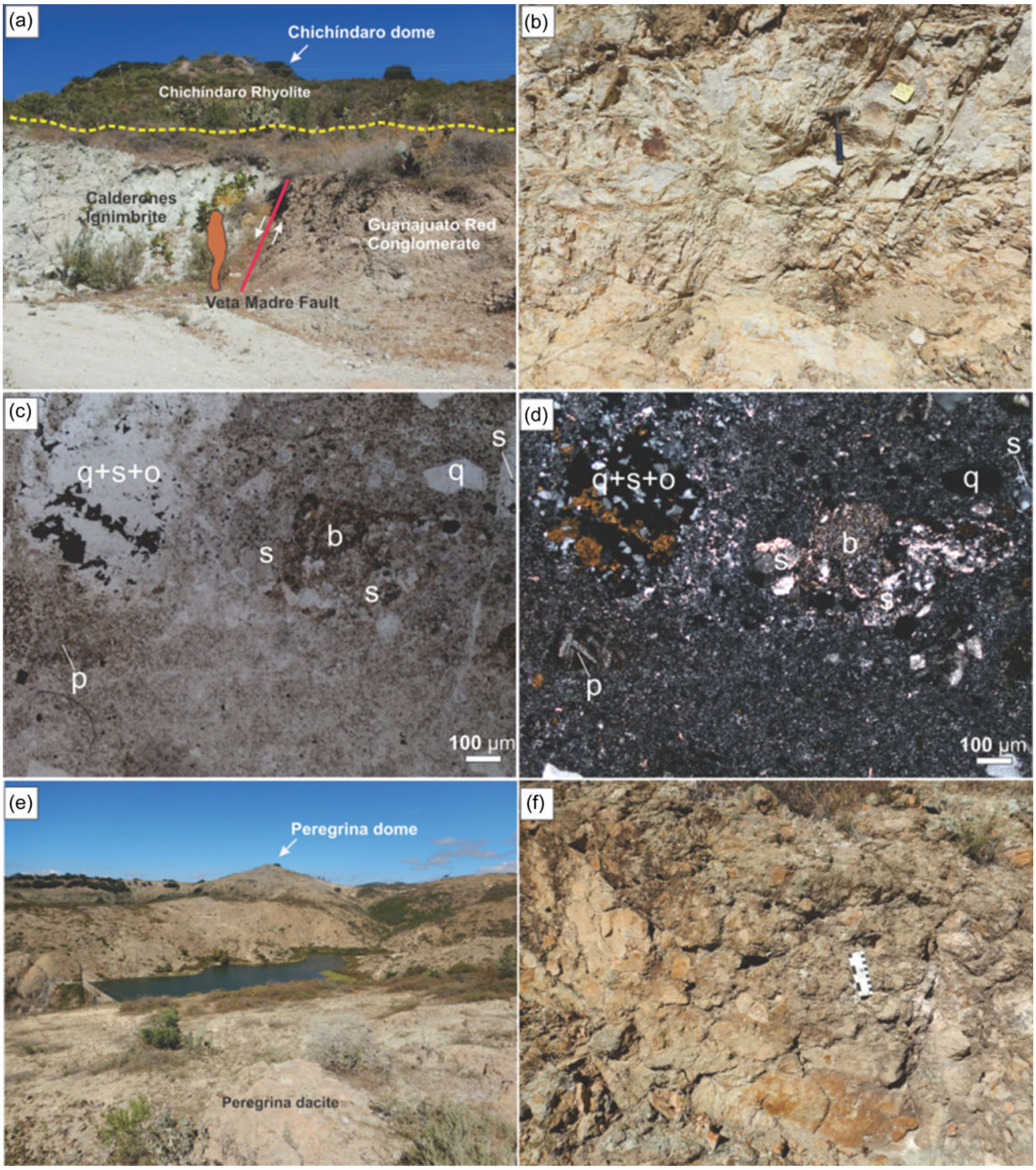

Figure 12. Images of Chichíndaro Formation. (a) Field photograph showing part of the Chichíndario dome in the distance (Cerro Chichíndaro). Chichíndaro rhyolite is in contact with the Calderones Ignimbrite and the Guanajuato Red Conglomerate that are in fault contact along the Veta Madre Fault (see Fig. 13 for a sketch profile). (b) Outcrop of the Chichíndaro rhyolitic lava showing semivertical dome foliation. (c) and (d) Photomicrographs of Chichíndaro lava, plain and polarized light, respectively, showing a porphyritic, hypocrystalline, devitrifed texture, with phenocrysts of sanidine (s), plagioclase (p), quartz (q), oxidized biotite (b) and Fe-Ti oxides due to alteration of the rock (o). (e) View of part of Peregrina dacitic dome, showing its aspect in the field. (f) Outcrop of lava auto breccia in the external part of the dome.

7. Discussion

7.a. Stratigraphic review

We have revised the stratigraphic sequence of the Guanajuato Mining District and have mapped in more detail the pre-caldera, syn-caldera and post-caldera units, documenting this revised stratigraphy with U-Pb zircon ages performed by us and with geochronologic data from other authors, with the conclusion that the Loseros, Bufa and Calderones units are concordant among them, that is, without any evidence of an important volcanic hiatus either sedimentary, paleosols or erosional, and thus, we propose that there are no unconformities between these units as have been reported previously (e.g., Echegoyén-Sánchez *et al.* 1970; Randall *et al.* 1994). In most sites, the sedimentary contacts are sharp and parallel, and in others, they are sharp but with some angularity due to the flow dynamics turbulent emplacement of the pyroclastic density currents. Furthermore, our U-Pb ages on zircon separates indicate that the Loseros-Bufa-Calderones sequence was emplaced within a short period, around 32.8 ± 0.2 Ma (Table 2). After a volcanic quiescence, activity restarted with the emplacement of the post-collapse domes, named here as El Rodeo and Chichíndaro formations, which are bounded by unconformities. All these units are here included in the Guanajuato Caldera Volcanic Group, in some agreement with

https://doi.org/10.1017/S0016756825100071 Published online by Cambridge University Press

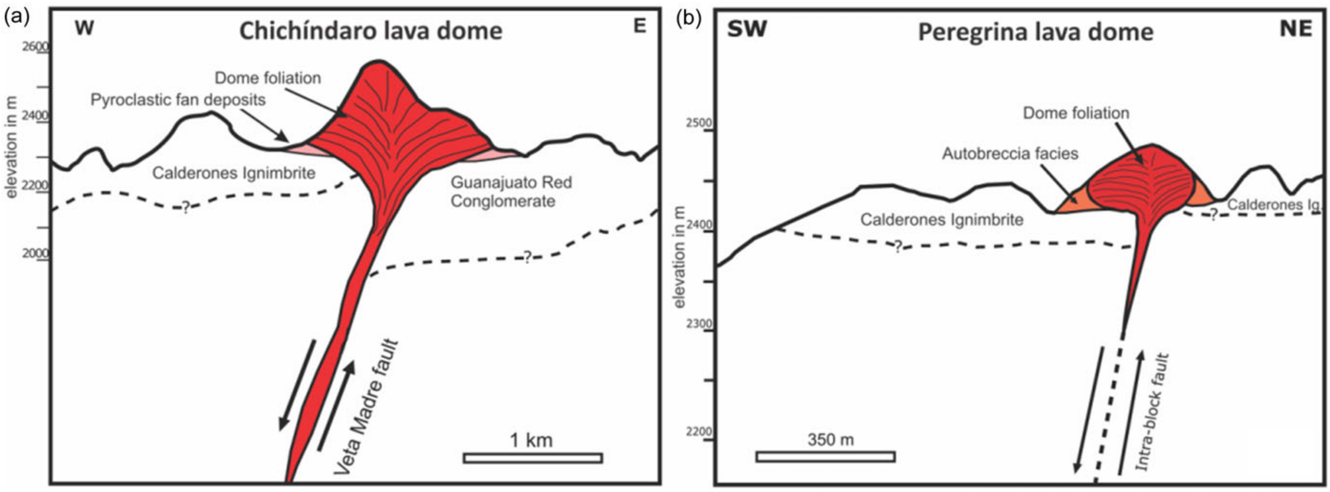

Figure 13. Schematic geologic profiles of post-collapse intra-caldera domes (modified from Randall *et al.* 1994). (a) Chichíndaro dome (Cerro Chichíndaro) emplaced over the Veta Madre fault. (b) Peregrina dome emplaced over an inferred fault apparently formed during caldera collapse.

the definition of Nieto-Samaniego *et al.* (2016), but we include, in the group, the post-caldera collapse domes, whereas these authors do not, and for now, we prefer to exclude the Cedro Andesite Formation because its relationship with the Guanajuato caldera magmatic system is uncertain.

Following the recommendation of Martí *et al.* (2018) for volcanic complexes or volcanic edifices, the re-organization of the stratigraphy of the Guanajuato Mining District presented here, and, particularly, of the units related with the Guanajuato graben caldera volcanic system allow a better understanding of the volcanic phases associated with the caldera formation, and that the Loseros-Bufa-Calderones pyroclastic series constitute a formation, named here the Guanajuato Pyroclastic Formation. With respect to the Guanajuato Red Conglomerate Formation, our field evidence shows that the sedimentary contact of this formation with Loseros PDCD Member is concordant and transitional; that is, the firsts PDCD of Loseros are interlayered with sand deposits of the uppermost part of the Guanajuato Red Conglomerate, indicating that when Loseros PDCs eruptions started there was still deposition of sands of the Guanajuato Red Conglomerate; thus, the initial PDCs of Loseros were probably deposited in a fluvio-lacustrine environment, perhaps in shallow water ponds, and further on as eruption continued, PDC pulses of Loseros were accumulated as subaerial deposits, without interlayered sand deposits. This concordant contact allows to date the upper limit of the Guanajuato Red Conglomerate at around 32.8 ± 0.1 which is the combined age of two dated samples of Loseros PDCD (Samples Gua-19 and Gua-32; Table 2). Despite Guanajuato Red Conglomerate is concordant with the Loseros PDCD member, the former does not form part of the volcanic system of Guanajuato graben caldera, and thus, it is a different formation, as was defined by other authors (e.g., Wandke & Martínez, 1928; Edwards, 1955; Randall *et al.* 1994).

7.b. The Guanajuato graben-type caldera

The volcanic sequence observed in the Guanajuato Mining District and the thick alluvial-fan sequence of the Guanajuato Red Conglomerate Formation, as well as the distribution of the pyroclastic units, Loseros, Bufa, and Calderones members, and of the distribution and age of the felsic lava domes of the area (El Rodeo and Chichíndaro formations; Fig. 3), suggest that the same tectonic depression was used to accommodate these thick sedimentary and volcanic successions (Figs. 7 and 15). As occurs in other volcano-tectonic depressions of the SMO (Aguirre-Díaz *et al.* 2008; Aguirre-Díaz *et al.* 2021), this points out towards the existence of a graben caldera in this sector, as was previously suggested (Aguirre-Díaz *et al.* 2012*a*, 2012*b*, 2013*a*, 2013*b*), rather than a classic semicircular ring-fracture-bounded caldera outlined by Randall *et al.* (1994). The caldera structure that we identified has a square shape (Figs. 3 and 15), with a size of 15 × 16 km and its subsidence was probably controlled by the NNW-SSE and ENE-WSW local fault systems, with the Sierra Vein System at the NE, the Aldana fault at the NW, and having the caldera faults of the SE and SW sides covered by the El Rodeo caldera margin domes, with the SW sector displaced by the El Bajío Fault (Figs. 3, 15, 17).

The observed caldera sequence in Guanajuato is similar to that reported for graben calderas (Aguirre-Díaz, 2008; Aguirre-Díaz *et al.* 2008, 2021; Aguirre-Díaz & Martí, 2015), including, from oldest to youngest, (1) alluvial-fan deposits represented here by the Guanajuato Red Conglomerate Formation, corresponding to the pre-caldera intra-graben fill during tectonic subsidence, (2) pyroclastic density currents (PDCs) deposits and large-volume ignimbrites with proximal vent co-ignimbrite lithic breccias, corresponding here to the Guanajuato Pyroclastic Formation, and (3) felsic lava domes emplaced along the caldera margin and inside the caldera, corresponding here to El Rodeo and Chichíndaro formations (Figs. 3, 4, 7, 13, 15 and 17).

Notably, Plinian fallout deposits are not observed in the caldera sequence (Fig. 7), which is a characteristic of graben-type calderas (Aguirre-Díaz *et al.* 2008, 2021; Aguirre-Díaz & Martí, 2015). Thus, the onset of caldera collapse represented by the major PDCs-forming ignimbrites must occur just after the deposition of continental sediments within the graben domain and a relatively low volume of dilute PDCs (Aguirre-Díaz *et al.* 2008, 2021). A similar volcano-tectonic development is observed

https://doi.org/10.1017/S0016756825100071 Published online by Cambridge University Press

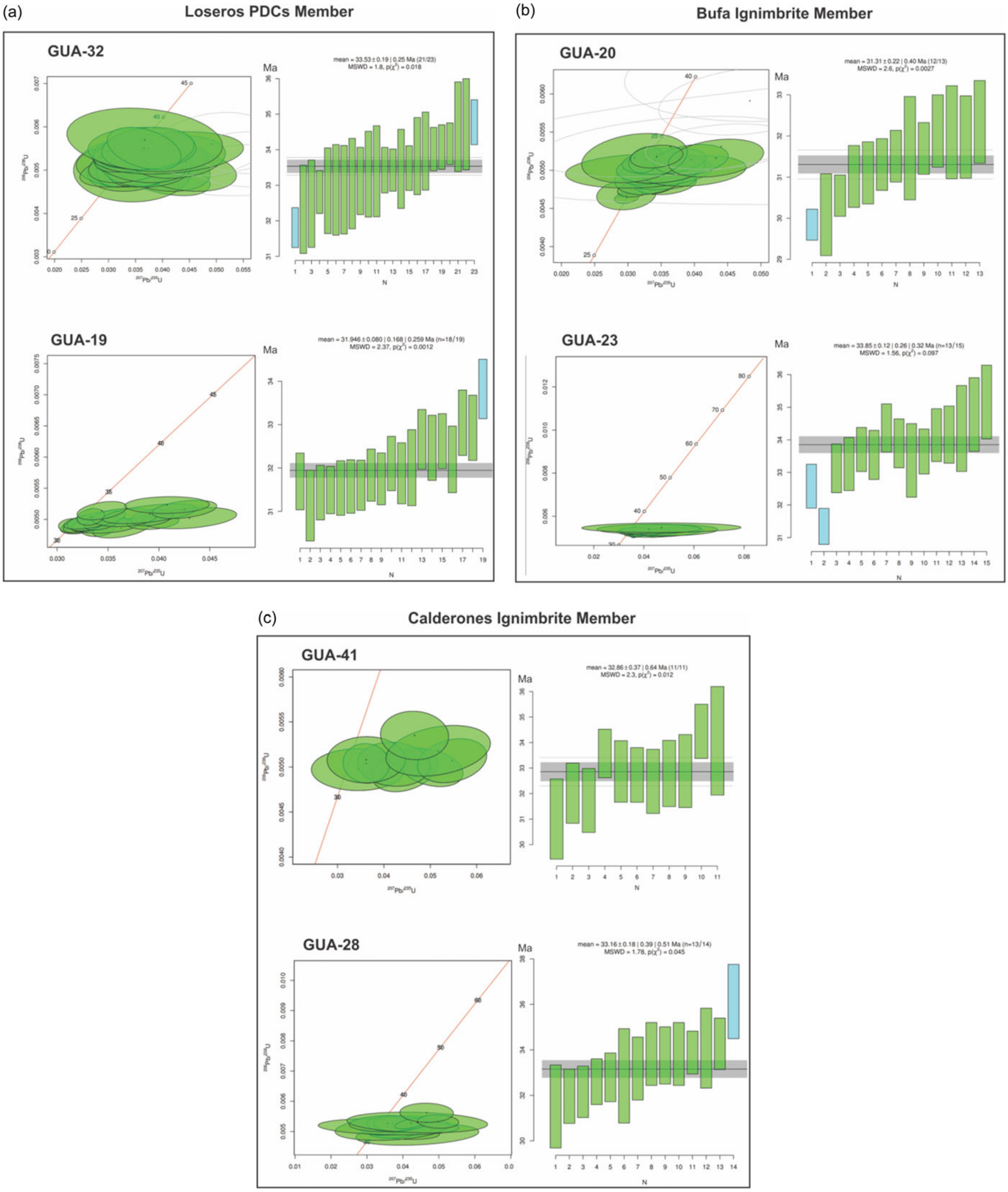

Figure 14. Graphs of the U/Pb age data performed on zircons for this study (Table 2). Full data tables are available as Supplementary Materials. (a) Graphs of Loseros PDCD member, (b) Graphs of Bufa Ignimbrite member, (c) Graphs of Calderones Ignimbrite member.

in graben or pull-apart basins in other places in the world (e.g., Martí, 1991; Molina-Zúñiga *et al.* 2014; Suñe-Puchol *et al.* 2019*a*, 2019*b*; Martí *et al.* 2023, 2024; Saura *et al.* 2025). Therefore, extensional or transtensional tectonics, before and during caldera collapse, and the emplacement of a sub-graben shallow silicic magma chamber are the necessary conditions for the development of graben calderas (Aguirre-Díaz, 2008; Aguirre-Díaz *et al.* 2008).

https://doi.org/10.1017/S0016756825100071 Published online by Cambridge University Press

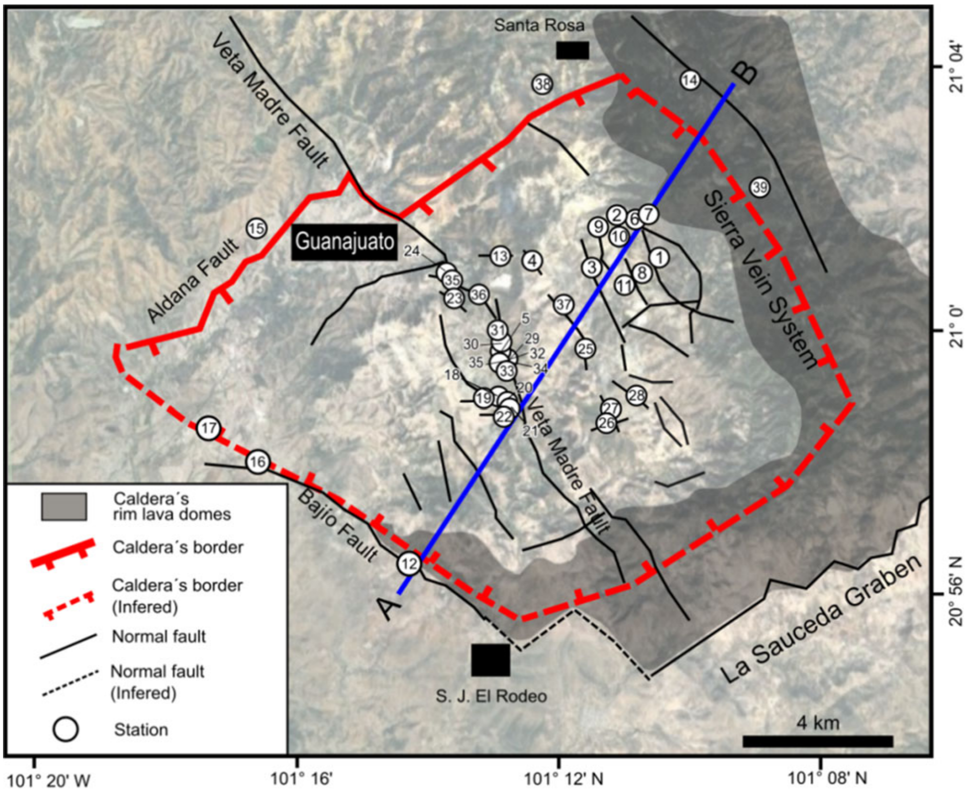

Figure 15. Simplified structural map of the Guanajuato graben caldera. Only main faults are shown for clarity. A-B line refers to the geologic cross-section shown in Fig. 17. Numbers in circles indicate the sites of fault measurements shown in Table 3.

7.c. Volcano-tectonic evolution of the Guanajuato graben caldera and resurgence

Volcanic activity initiated with Loseros dilute PDCs and was immediately followed by the emplacement of dense PDCs that formed the Bufa Ignimbrite (Fig. 18). Loseros PDCs may be considered as a restricted vent opening phase that helped the magma chamber start decompression of volatiles, initial evacuation of magma, and acquire stress conditions to favour caldera collapse (Fig. 18d). The Loseros PDCD are mainly characterized by their fine grain size and thin laminations, indicating a phreatomagmatic origin that resulted in a high degree of fragmentation in these first eruptive pulses. This is also supported by the fact that Loseros was initially deposited in a shallow subaqueous environment or ponds, at least for the first deposits in contact with the Guanajuato Red Conglomerate. However, these conditions rapidly changed to a subaerial environment in the upper beds of Loseros PDCD; thus, the humid conditions finished quickly. The 'ondulites' reported elsewhere may suggest strong seismicity on soft humid deposits that could have been associated with the caldera activity; that is, seismite structures.

Just after Loseros diluted PDCD were emplaced, and without any time break, the eruption turned into massive proportions forming the Bufa Ignimbrite and allowing the gravitational collapse of crustal blocks inside the magma chamber while this was progressively decompressing (Fig. 18e). Co-ignimbrite lithic lag breccias corresponding to major pulses of vent opening (e.g., Walker, 1985; Aguirre-Díaz *et al.* 2021) are evident in several places within the Bufa and Calderones ignimbrites. Lithics in these breccias are mostly of Mesozoic basement lithologies, including schists, andesitic and rhyolitic lavas, several types of intrusive rocks, and of the Guanajuato Red Conglomerate. These types of breccias occur next to their corresponding vents, in this case, next to the normal faults of the intra-caldera collapsed blocks and the main faults that delimit the caldera of Guanajuato (Figs. 3 and 4). Therefore, the vents for Bufa Ignimbrite were probably fissures, as Aguirre-Díaz and Labarthe-Hernández (2003) suggested for the formation of the large-volume ignimbrites of the SMO, and used the intra-caldera block faults and the caldera bordering faults as conduits that were connected to the subcaldera magma chamber, as proposed for graben-type calderas (Aguirre-Díaz, 2008; Aguirre-Díaz *et al.* 2008, 2021).

After the emplacement of the Bufa Ignimbrite the eruption continued, without stopping, in the form of pulsating PDCs and the formation of the Calderones Ignimbrite (Fig. 18f). As in Bufa Ignimbrite, the vents were probably fault-controlled fissures. The concordant contact between Calderones and Bufa as well as the absence of paleosols, erosional or sedimentary features between them indicate that the caldera activity did not stop between both eruption phases. Calderones sequence started with more dilute, lithics-rich PDCs that changed with time to more massive and denser PDCs ending with at least three massive ignimbrites, as shown in the site of Cerro La Loca (Fig. 7). This suggests that there was a change in the eruption conditions between Bufa (massive proportions) to the first stages of Calderones, where mass output rate decreased substantially but progressively increased again towards the last Calderones unit pulses. This could explain the layered characteristic of Calderones Ignimbrite, with thin bedding at the base, to intermediate thickness at the middle, and thickest (3–10 m) ignimbrites at the top (Fig. 10a, b). Another characteristic of the Calderones unit is the abundance of lithics in most deposits, with some beds classifying as co-ignimbrite lithic lag breccias when they are associated with the more massive deposits, or thin breccia-surge deposits if they were formed from dilute PDCs (Fig. 10c, d).

https://doi.org/10.1017/S0016756825100071 Published online by Cambridge University Press

Table 3. Structural data of major faults of the Guanajuato graben caldera

Station	Fault #	Fault name	Strike	Dip	Azimuth	North*	East*
1	1	Villalpando	S 45° E	55°	135	2325266.1	2,73,760.8
2	2	Villalpando del Alto	S 77° E	50°	103	2326213.4	2,72,871.6
3	3	El Cubo	S 60° E	40°	120	2324840.4	2,72,180.9
4	4	La Leona	S 35° E	53°	155	2325062.6	2,70,612.8
5	5	Veta Madre	S 19° E	45°	161	2322543.2	2,69,842.6
6	6	Soledad	N 45° W	55°	315	2326139.9	2,73,329.2
7	7	San Miguel	N 70° W	45°	290	2326169.4	2,73,394.3
8	8	Capulín	S 30° E	64°	150	2324658.3	2,73,451.0
9	9	Dolores	S 45° E	50°	135	2325646.2	2,72,478.5
10	10	La Loca-1	S 20° E	70°	160	2325743.9	2,72,837.6
11	11	San Eusebio	S 55° E	70°	125	2324500	2,73,000.0
12	12	El Bajío	S 55° E	70°	125	2316929.6	2,67,212.6
13	13	Las Escobas	S 78° E	68°	102	2325204.6	2,69,758.9
14	14	Peralillo	N 77° W	70°	283	2330117.8	2,74,622.3
15	15	Aldana	N 45° E	55°	45	2326160.3	2,63,218.0
16	16	Yerbabuena-Bufa	N60°W	60°	300	2319800	2,63,188.0
	17	Yerbabuena-Bufa	S50°W	60°	230	2319800	2,63,188.0
	18	Yerbabuena-Bufa	N70°W	75°	290	2319800	2,63,188.0
17	19	Yerbabuena-Bufa	S50°W	80°	230	2320733	2,62,048.0
	20	Yerbabuena-Bufa	N25°W	55°	335	2320733	2,62,048.0
18	41	El Carmen-Santo Niño	S05°E	90°	175	2321420	2,69,603.0
19	42	El Carmen-Santo Niño	W	70°	270	2321459	2,69,357.0
	43	El Carmen-Santo Niño	N	90°	0	2321459	2,69,357.0
20	44	El Carmen-Santo Niño	S10°E	55°	170	2321252	2,69,888.0
	45	El Carmen-Santo Niño	S50°E	70°	130	2321252	2,69,888.0
21	46	El Carmen-Santo Niño	N10°W	80°	350	2321109	2,69,940.0
22	47	El Carmen-Santo Niño	E	75°	90	2320980	2,69,823.0
	48	El Carmen-Santo Niño	S35°E	50°	145	2320980	2,69,823.0
	49	El Carmen-Santo Niño	S20°E	65°	160	2320980	2,69,823.0
	50	El Carmen-Santo Niño	S	55°	180	2320980	2,69,823.0
23	60	Santo Niño-Veta Madre	N35°W	55°	325	2324109	2,68,503.0
	61	Santo Niño-Veta Madre	N50°W	50°	310	2324109	2,68,503.0
	62	Santo Niño-Veta Madre	N60°W	45°	300	2324109	2,68,503.0
24	63	Santo Niño-Veta Madre	S25°E	80°	155	2324793	2,68,334.0
25	82	Mesa de Veta Grande	S25°W	65°	205	2322703	2,71,962.0
	83	Mesa de Veta Grande	S20°E	70°	160	2322703	2,71,962.0
26	84	Veta Madre-Nayal	S55°W	85°	235	2320928	2,72,506.0
	85	Veta Madre-Nayal	N60°W	45°	300	2320928	2,72,506.0
27	86	Veta Madre-Nayal	S20°E	55°	160	2321083	2,72,597.0
28	87	Rosa de Castilla-Presa de jales el Nayal	S70°E	45°	110	2321407	2,73,303.0
	88	Rosa de Castilla-Presa de jales el Nayal	S50°E	60°	130	2321407	2,73,303.0
29	104	Barreno-Camino al Nayal	S50°E	80°	130	2322749	2,69,797.0
30	105	Barreno-Camino al Nayal	N70°W	75°	290	2322839	2,69,772.0

(*Continued*)

https://doi.org/10.1017/S0016756825100071 Published online by Cambridge University Press

Table 3. (*Continued*)

Station	Fault #	Fault name	Strike	Dip	Azimuth	North*	East*
	106	Barreno-Camino al Nayal	N85°W	60°	275	2322839	2,69,772.0
	107	Barreno-Camino al Nayal	N30°W	65°	330	2322839	2,69,772.0
	108	Barreno-Camino al Nayal	S40°E	60°	140	2322839	2,69,772.0
31	109	Barreno-Camino al Nayal	S80°E	70°	100	2322865	2,69,746.0
	110	Barreno-Camino al Nayal	S10°E	65°	170	2322865	2,69,746.0
32	111	Barreno-Camino al Nayal	S40°E	80°	140	2322697	2,69,733.0
33	112	Barreno-Camino al Nayal	S30°E	80°	150	2322152	2,69,888.0
	113	Barreno-Camino al Nayal	S45°E	60°	135	2322152	2,69,888.0
	114	Barreno-Camino al Nayal	N85°E	90°	85	2322152	2,69,888.0
34	115	Barreno-Camino al Nayal	S15°E	70°	165	2322476	2,69,953.0
	116	Barreno-Camino al Nayal	N05°W	80°	355	2322476	2,69,953.0
	117	Barreno-Camino al Nayal	N29°W	70°	331	2322476	2,69,953.0
35	118	Barreno-Camino al Nayal	N25°W	50°	335	2322412	2,69,862.0
	119	Barreno-Camino al Nayal	S30°E	20°	150	2322412	2,69,862.0
36	120	Oriente de Gto	S85°W	70°	265	2324589	2,68,450.0
	121	Oriente de Gto	S35°E	60°	145	2324589	2,68,450.0
	122	Oriente de Gto	S60°E	60°	120	2324589	2,68,450.0
37	123	Oriente de Gto	N50°E	70°	50	2324433	2,68,709.0
38	124	Oriente de Gto	S56°E	53°	124	2324174	2,69,175.0
39	125	Poniente de Mineral del Cubo	S50°E	57°	130	2323869	2,71,411.0
	126	Poniente de Mineral del Cubo	S50°E	65°	130	2323869	2,71,411.0
	127	Poniente de Mineral del Cubo	S35°E	30°	145	2323869	2,71,411.0
	128	Poniente de Mineral del Cubo	S48°E	70°	132	2323869	2,71,411.0
40	129	La Loca-2	N05°W	50°	355	2324654	2,73,083.0
41	130	San Nicolas	N45°E	85°	45	2329876	2,70,912.0
42	131	SE Sta Rosa	N40°W	55°	320	2326980	2,76,543.0
43	132	SE Sta Rosa	S20°E	85°	160	2327148	2,76,627.0
44	133	SE Sta Rosa	N70°W	70°	290	2327044	2,76,439.0
	134	SE Sta Rosa	N65°W	60°	295	2327044	2,76,439.0

Azimuth of strike; *UTM coordinates using datum NAD27.

Therefore, the eruption style changed from Bufa to Calderones, but both styles forming part of a single caldera collapse event; the former was associated with a massive extraction of magma from the chamber probably during a paroxysmal caldera collapse phase, while the latter suggests an unsteady and pulsating eruption phase probably related to a stage of discontinuous caldera collapse that produced an irregular extraction of magma from the chamber with an increase of the mass flow rate with time. As in the Bufa Ignimbrite, the co-ignimbrite lithic lag breccias of Calderones deposits crop out next to the intra-caldera collapsed blocks, as well as next to the major faults that make the structural limits of the Guanajuato caldera (Figs. 3, 4 and 7). A notorious case is the locality with co-ignimbrite megabreccias exposed near Peregrina mine at the western flank of Cerro de Villalpando (Fig. 10d, g, h), which apparently resulted from the caldera wall collapse during the eruption that formed Calderones Ignimbrite. Most outcrops of ignimbrite lithic breccias occur within the caldera limits, mainly because of erosion of practically all the outflow facies, but in few localities, proximal outflow facies were preserved, such as in Cerro San Nicolás, at the NE margin of the caldera (Fig. 3). In these outflow facies, it is common to observe blocks with ballistic impacts indicating that they were ejected from the caldera border, in this case, related with Cerro San Nicolás marginal fault. As in Bufa Ignimbrite, no Plinian phase eruption is evident in the Calderones deposits, which is a characteristic of graben-type calderas (Aguirre-Díaz, 2008; Aguirre-Díaz *et al.* 2008).

At about 31 Ma, the style of volcanism changed from explosive to effusive, and several lava domes were emplaced along the caldera's marginal faults (Fig. 18h). Magma used the same PDCs fissure conduits to form a chain of felsic domes that are better preserved along the SW and the NE margins, corresponding to the El Rodeo Formation (Figs. 3, 15 and 17). The same style of post-collapse dome emplacement has been observed in other graben calderas of the SMO; for instance, at Bolaños caldera (Aguirre-Díaz

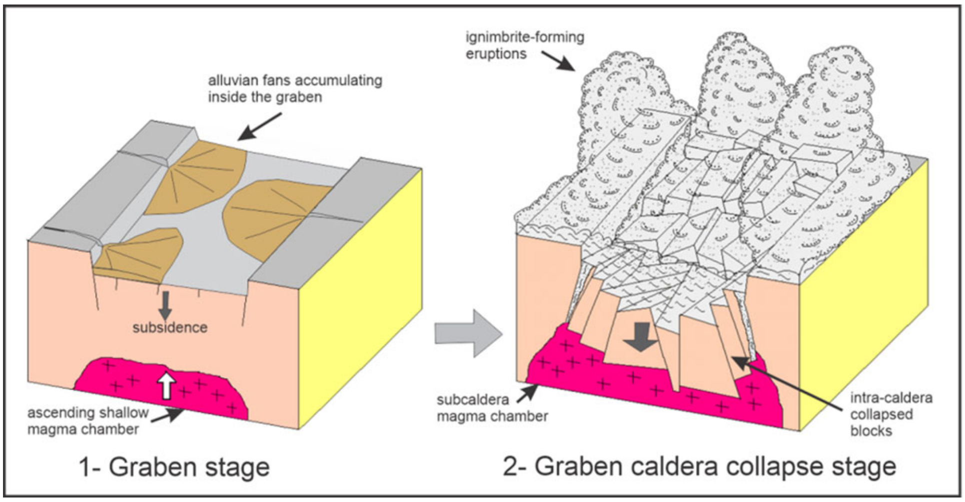

Figure 16. Schematic conceptual model for the development of a graben-type caldera. Stage 1- pre-existing graben conditions with accumulation of continental sedimentary deposits (alluvial fans) during tectonic subsidence; at the same time, a shallow magma chamber is ascending towards the graben, with the corresponding increasing in magmatic pressure due to depressurization and volatile exsolution. Stage 2- interaction of the graben faults with the top of the over pressurized magma chamber, opening of the system, massive ignimbrite-forming eruptions and caldera collapse.

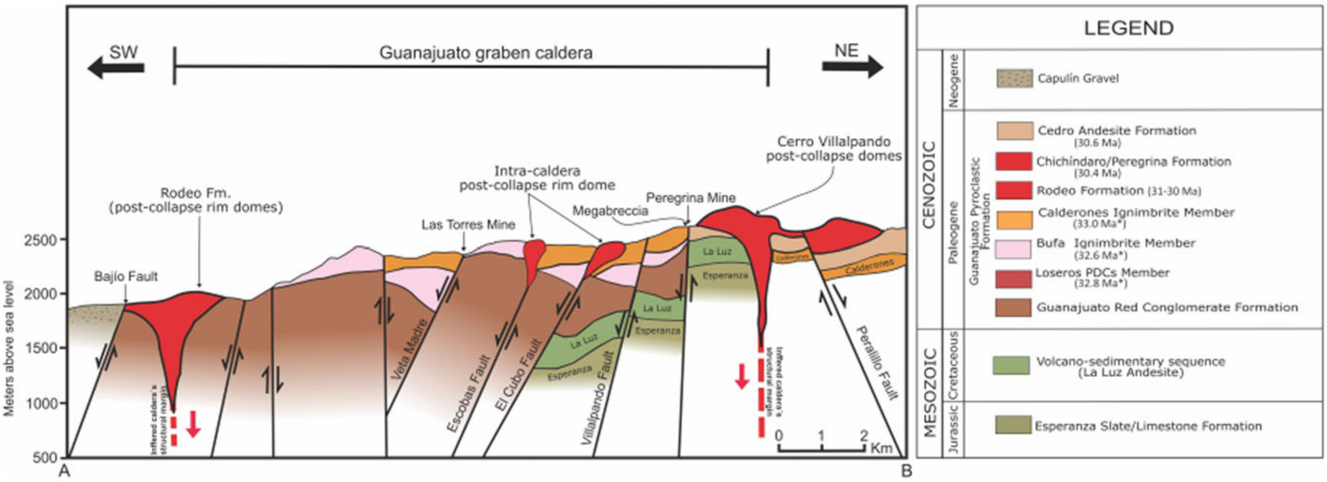

Figure 17. Geologic cross-section across the Guanajuato graben caldera along A-B line in the geologic and structural maps, Figures 3 and 15. The marginal faults of the caldera are inferred beneath the rim lava domes (El Rodeo Formation) that apparently were emplaced after the caldera collapse and used these faults as vents. Based on Randall *et al.* (1994)'s cross-sections and our own observations.

et al. 2021), and is a common phase in calderas in general (e.g., Bailey *et al.* 1976: Mahood, 1980; Aguirre-Díaz & McDowell, 2000; Ashwell *et al.* 2013).

Resurgence of the caldera may have occurred simultaneously with emplacement of the post-collapse intra-caldera lava domes, apparently caused by a last upward pulse of remnants of felsic magma in the magma chamber (Fig. 18h). This pulse had two major effects in the caldera area; (1) push-up of the intra-caldera collapsed blocks and of the caldera fill deposits, including the Guanajuato Red Conglomerate and the Guanajuato Pyroclastic formations; and (2), these formations were affected by new faults probably influenced by the buried intra-blocks faults formed during the caldera collapse, so that the faults that bound the intra-caldera blocks had at least two displacement episodes, one caused by the caldera collapse, and another caused by the resurgence phase, plus tectonic activity that may have affected the region after the Oligocene. The result is a complex fault displacement scenario in the Guanajuato Mining District area that also displaced the Guanajuato Pyroclastic Formation. The resurgence phase uplifted the caldera floor, which is represented by the Guanajuato Red Conglomerate and its contact with the Guanajuato Pyroclastic Formation; this contact was moved up closer to the surface and, after a 31 Ma lasting erosion, the caldera floor is now exposed (Fig. 18i), which can be observed at several sites within the caldera, particularly, at and around Guanajuato City (Fig. 3). Erosion removed a large portion of the Guanajuato caldera products, leaving remnants of them mainly in the intra-caldera facies, such as Cerro La Bufa and Cerro La Loca sites (Fig. 7). This erosion process was facilitated by uplifting caused by the proposed resurgence.

This resurgence phase has not been reported before for the Guanajuato caldera, but it could be a key phase to explain the uplifting of the caldera floor, represented by the sedimentary contact of the Guanajuato Red Conglomerate and the Loseros PDCD Member, and with other members of the Guanajuato Pyroclastic Formation. After a long-term erosion of about 31 Ma, it is now possible to observe the caldera floor at the surface.

https://doi.org/10.1017/S0016756825100071 Published online by Cambridge University Press

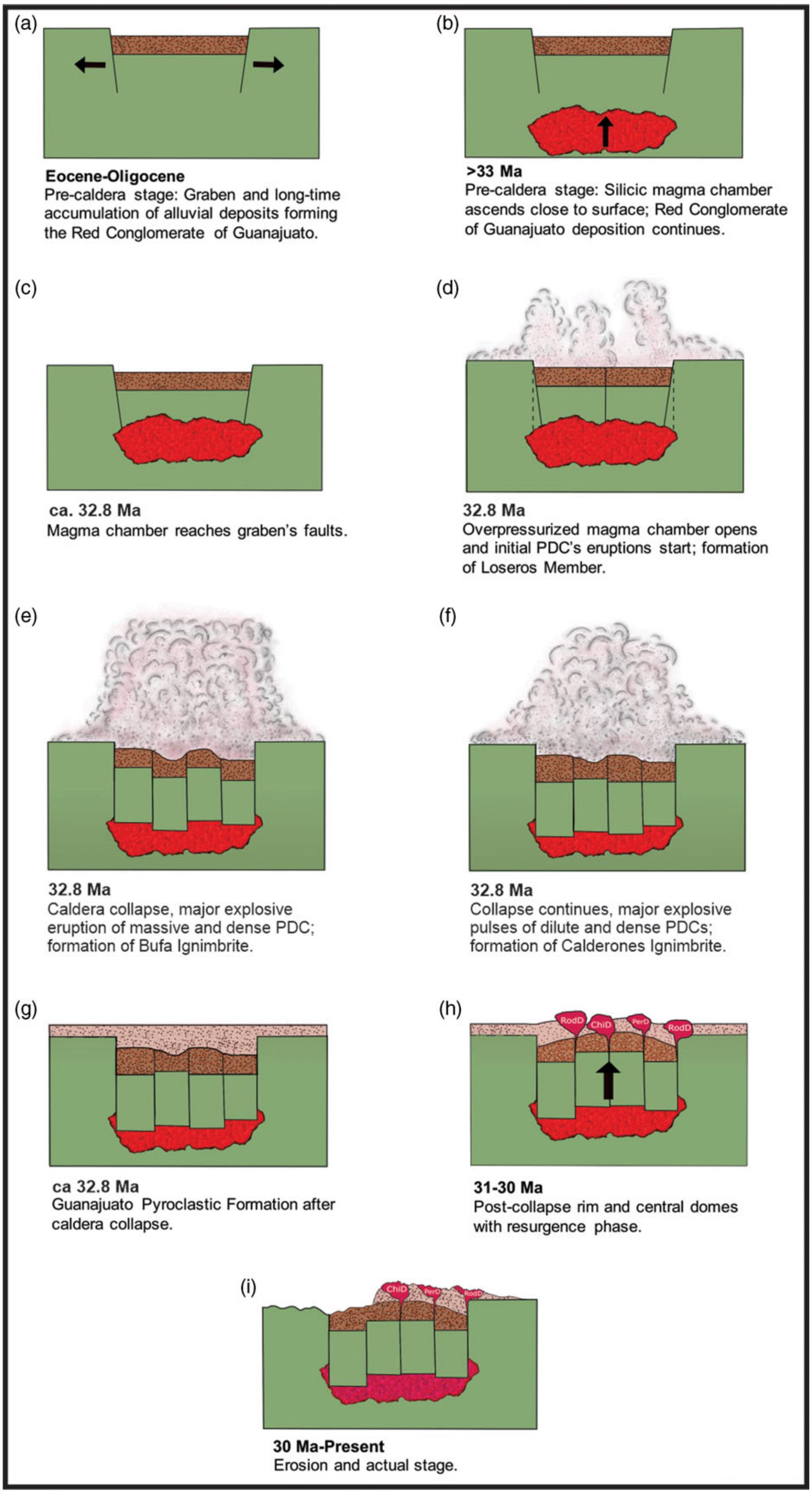

Figure 18. Volcanic evolution of the Guanajuato graben caldera showing the different phases, including the pre-caldera graben stage, the caldera formation and major ignimbrites, the post-collapse resurgence and dome emplacement, and the actual stage after erosion.

Resurgence also explains the complex fault displacements observed within the caldera, since the faults bounding the intra-caldera collapsed blocks were first displaced downwards with the gravitational collapse, and later upwards with the resurgence, and were probably reactivated by more recent regional tectonic events of the area younger than 31 Ma.

8. Conclusions

We can conclude from our geological observations and geochronological results that the mid-Tertiary volcanic stratigraphy in the Guanajuato Mining District corresponds to a caldera-forming succession and that the resulting Guanajuato caldera developed under a tectonic extensional control. The Guanajuato caldera succession, formed within 32.8–30.0 Ma, follows the general sequence observed in graben-type calderas of the SMO, which are characterized by a pre-caldera alluvial-fan and/or lacustrine graben fill, absence of Plinian column pyroclastic deposits in the initial volcanic stages, and a series of caldera-forming PDC deposits, mainly ignimbrites, ending with the emplacement of post-collapse domes. In Guanajuato's case, from base to top, the sequence includes (1) at least 2,000 m of alluvial fan deposits within a tectonic basin that resulted in the Eocene-Oligocene Guanajuato Red Conglomerate Formation; (2) An initial volcanic activity of diluted pyroclastic density currents that formed the Loseros PDC deposits at about 32.8 ± 0.1 Ma; (3) A major caldera collapse episode in which magma was extracted explosively in massive proportions represented here by two different but successive units, the Bufa and the Calderones ignimbrites, at about 32.8 ± 0.2 Ma; and (4) effusive volcanism in the form of rhyolitic and dacitic lava domes, represented by the El Rodeo caldera rim domes and the Chichíndaro-Peregrina intra-caldera domes, dated by other authors at 31–30 Ma. Contemporaneous with this last dome event, the caldera could have had a resurgence phase that uplifted the caldera floor. We revised the nomenclature of the units following a volcanic stratigraphic code linked to a volcanic edifice or system, in this case, the Guanajuato graben caldera, proposing the names of Guanajuato Pyroclastic Formation that includes the Loseros, Bufa and Calderones members, El Rodeo Formation for the caldera rim domes, and the Chichíndaro Formation that includes the intra-caldera felsic domes best represented by the Chichíndaro and Peregrina domes. All these units together form the Guanajuato Caldera Volcanic Group.

Supplementary material. The supplementary material for this article can be found at https://doi.org/10.1017/S0016756825100071

Acknowledgements. We thank Carlos Ortega for his assistance in zircon U-Pb dating at Instituto de Geociencias (IGC) of Universidad Nacional Autónoma de México (UNAM), and to Juan Tomás Vásquez for the elaboration of thin sections also at the IGC-UNAM. We acknowledge the careful review of this work by the anonymous referees and Prof Olivier Lacombe, Geological Magazine's editor, whose comments improved the manuscript. This study was possible thanks to the DGAPA-PAPIIT-UNAM grants IN112312 and IN108621 to the first author, and a scholarship from the first project to Mariana Coutiño-Taboada, to the DGAPA-PAPIME-UNAM grants PE101816 and PE102419, and to grants from the International Academic Interchange Program of the Coordinación de la Investigación Científica - CIC-UNAM in 2021, 2022 and 2023. We also thank to the Ministerio de Ciencia e Innovación del Gobierno de España for the grant PID2020-114273GB-C21, MACIN Project.

References

Aguirre-Díaz GJ (2008) Types of collapse calderas. *IOP Conference Series: Earth and Environmental Science* **3**, 012021.

Aguirre-Díaz GJ, Coutiño-Taboada ME, Martínez-Reyes JJ and Ortega-Obregón C (2016) New U-Pb zircon ages in the Guanajuato Mining District and comparison with previous K-Ar and ^{40}Ar-^{39}Ar ages: Evidence for a major caldera eruption. *South American Symposium on Isotope Geology (SSAGI10th)*, May 2225, 2016, Puerto Vallarta, Mexico. www.ssagi10.geofisica.unam.mx.

Aguirre-Díaz GJ, Ferrari L, Nelson SA, Carrasco-Núñez G, López-Martínez M and Urrutia-Fucugauchi J (1998) El Cinturón Volcánico Mexicano: Un Nuevo Proyecto Multidisciplinario. *Unión Geofísica Mexicana Geos* **18**, 131–138. http://www.ugm.org.mx/publicaciones/geos/geos1998.html.

Aguirre-Díaz GJ and Labarthe-Hernández G (2003) Fissure ignimbrites: fissure-source origin for voluminous ignimbrites of the Sierra Madre Occidental and its relationship with Basin and Range faulting. *Geology* **31**, 773–76.

Aguirre-Díaz GJ, Labarthe-Hernández G, Tristán-González M, Nieto-Obregón J and Gutiérrez-Palomares I (2008) Ignimbrite Flare-up and graben-calderas of the Sierra Madre Occidental, Mexico. In *Caldera Volcanism: Analysis, Modelling and Response* (eds J Gottsmann & J Martí), pp. 143–180. Amsterdam: Elsevier.

Aguirre-Díaz GJ and Martí J (2015) Graben calderas: Examples from Mexico, Central America, and the Andes. *26th IUGG General Assembly, Prague, Czech Republic*, 2, 2015. https://www.czech-in.org/cm/IUGG/CM.NET.

Aguirre-Díaz GJ and Mcdowell FW (1993) Nature and Timing of faulting and syn-extensional magmatism in the southern Basin and Range, central-eastern Durango, Mexico. *Bulletin of the Geological Society of America* **105**, 1435–1444. https://doi.org/10.1130/0016-7606(1993)105<1435:NATOFA>2.3.CO;2.

Aguirre-Díaz GJ and Mcdowell FW (2000) Volcanic evolution of the Amealco caldera, central Mexico. In *Cenozoic Tectonics and Volcanism of Mexico* (eds H Delgado-Granados, J Stock, & GJ Aguirre-Díaz). *Geological Society of America Special Paper* **334**, 167–78. https://doi.org/10.1130/0-8137-2334-5.179.

Aguirre-Díaz GJ and McDowell FW (1991) The volcanic section at Nazas, Durango, Mexico, and the possibility of widespread Eocene volcanism within the Sierra Madre Occidental. *Journal of Geophysical Research* **96**, 373–88.

Aguirre-Díaz GJ, Tristán-González M, Gutiérrez-Palomares I, Martí J, López-Martínez M, Labarthe-Hernández G and Nieto-Obregón J (2021) Graben-type calderas: the Bolaños case, Sierra Madre Occidental, Mexico. *Journal of Volcanology and Geothermal Research* **417**, 107315.

Aguirre-Díaz GJ, Tristán-González M, Labarthe-Hernández G and Martí J (2013a) The graben caldera of Guanajuato, Mexico. *AGU Meeting of the Americas, Cancun, México 2013 Abstracts* V43A-04, http://abstractsearch.agu.org/meetings/2013/JA/V43A-04.html.

Aguirre-Díaz GJ, Tristán-González M, Labarthe-Hernández G and Martí J (2013b) Graben calderas of the Sierra Madre Occidental: the case of Guanajuato, central Mexico. *AGU Fall Meeting 2013, San Francisco, Eos*, **94**, V23A–2781. http://abstractsearch.agu.org/meetings/2013/FM/V23A2781.html

Aguirre-Díaz GJ, Tristán-González M, Martí J and Labarthe-Hernández G (2014) Revised stratigraphy of the Guanajuato Mining District, central Mexico: Geological evidence for a graben type collapse caldera. *1st. IAVCEI Workshop on Volcanic Geology, Funchal, Madeira, Portugal, Abstracts*, pp 4. http://www.iavcei.org/IAVCEI_meetings/MADEIRA/Workshop_Volcano_Geology/.

Aguirre-Díaz GJ, Tristán-González M, Martí J, Martínez-Reyes JJ and Labarthe-Hernández G (2012b) The ignimbrite sequence of Guanajuato, Mexico: Evidence of a collapse caldera in the southern Sierra Madre Occidental. IAVCEI 4th International Workshop on Collapse Calderas, Bolsena, Italy.

Aguirre-Díaz GJ, Tristán-González M, Martí J, Martínez-Reyes JJ, Labarthe-Hernández G and Sánchez-Aguilar D (2012a) The Oligocene succession of Guanajuato, Mexico: a review from a volcanological approach. *Reunión Anual Unión Geofísica Mexicana 2012, Geos* **32**, 126.

Alquiza P and Avilés R (2015) Cenozoic seismites and soft-sediment deformation structures in the Losero Formation, southern Sierra de Guanajuato, Mexico. *Revista Mexicana de Ciencias Geológicas* **32**, 203–18.

Andrews GDM, Busby CJ, Brown SR, Fisher CM, Davila-Harris P, Strickland A, Vervoort JD, Pettus HD, McDowell FW and Murray BP (2022) Petrogenesis of voluminous silicic magmas in the Sierra Madre Occidental large igneous province, Mexican Cordillera: insights from zircon and Hf-O isotopes. *Geosphere* **18**, 946–84.

Aranda-Gómez J, Davila-Harris P, Vassallo-Morales L, Godchaux M, Bonnichsen B, Martínez-Reyes J, Aguirre-Díaz G and Ortega A (2012) Geology and tectonics of the southeastern portion of the Sierra de Guanajuato. *Geological Society of America Field Guide* **25**, 135–62.

Aranda-Gómez JJ, Godchaux MM, Aguirre-Díaz GJ, Bonnichsen B and Martínez-Reyes J (2003) Three superimposed volcanic arcs in the southern Cordillera – From the early Cretaceous to the Miocene, Guanajuato, Mexico. In *Geologic transects across Cordilleran Mexico, Guidebook for field trips of the 99th Annual Meeting of the Cordilleran Section of the Geological Society of America*, Mexico, D.F., Universidad Nacional Autónoma de México, *Instituto de Geología, Publicación Especial 1, Field Trip* 6, pp. 123–168.

Aranda-Gómez JJ and McDowell FW (1997) Extensión temprana en la porción meridional de la provincia de Cuencas y Sierras de México: Basculamiento contemporáneo al depósito de la secuencia terciaria (Eoceno-Oligoceno) del Distrito Minero de Guanajuato. *Proceedings Geos, Annual Meeting of the Unión Geofísica Mexicana* **17**, 225–26.

Ashwell PA, Kennedy BM, Gravley DM, von Aulock FW and Cole JW (2013) Insights into caldera and regional structures and magma body distribution from lava domes at Rotorua Caldera, New Zealand. *Journal of Volcanology and Geothermal Research* **258**, 187–202.

Atwater T (1989) Plate tectonic history of the northeast Pacific and western North America. In *The Eastern Pacific Ocean and Hawaii* (eds EL Winterer, DM Hussong & RW Decker), pp. 21–71. Boulder, Colorado: Geological Society of America

Atwater TA (2022) Plate Tectonic History of the North Pacific Ocean. Available at https://animations.geol.ucsb.edu/2_infopgs/IP3RegTect/dNoPacific.html (accessed 1 May 2025).

Bailey RA, Dalrymple GB and Lanphere MA (1976) Volcanism, structure, and geochronology of Long Valley caldera, Mono County, California. *Journal of Geophysical Research* **81**, 725–44.

Campa MF and Coney PJ (1983) Tectono-stratigraphic terranes and mineral resource distributions in Mexico. *Canadian Journal of Earth Sciences* **20**, 1040–51.

Centeno-García E, Guerrero-Suastegui M and Talavera-Mendoza O (2008) The Guerrero Composite Terrane of western Mexico: collision and subsequent rifting in a suprasubduction zone. In *Formation and Applications of the Sedimentary Record in Arc Collision Zones* (eds A Draut, PD Clift & DW Scholl), pp. 279–308. Boulder, Colorado: Geological Society of America.

Cerca-Martínez M, Aguirre-Díaz GJ and López-Martínez M (2000) The geologic evolution of southern Sierra de Guanajuato, Mexico: a documented example of the transition from the Sierra Madre Occidental to the Mexican Volcanic Belt. *International Geology Review* **12**, 131–51.

Coutiño-Taboada ME (2015) Correlación estratigráfica de las unidades del Terciario medio del Distrito Minero de Guanajuato, Gto. *Tesis Licenciatura Departamento de Ingeniería en Minas, Metalurgia y Geología, Escuela de Minas*, Universidad Autónoma de Guanajuato, Guanajuato, 66 p. http://repositorio.ugto.mx/handle/20.500.12059/7934.

Del Río P, Nieto-Samaniego A, Alaníz-Álvarez S, Ángeles-Moreno E, Escalona-Alcázar F and Del Pilar-Martínez A (2020) Geología y estructura de las sierras de Guanajuato y Codornices, Mesa Central, México. *Boletín de la Sociedad Geológica Mexicana* **72**, A071019.

Echegoyén-Sánchez J, Romero-Martínez S and Velázquez-Silva S (1970) Geología y yacimientos minerales de la parte central del Distrito Minero de Guanajuato. *Consejo de Recursos Naturales No Renovables Boletín* **75**, 36.

Edwards JD (1955) Studies on some early tertiary red conglomerates of central Mexico. *U.S. Geological Survey Professional Paper* **264–H**, 153–185.

Ferrari L, López-Martínez M, Aguirre-Díaz GJ and Carrasco-Núñez G (1999) Space-time patterns of Cenozoic arc volcanism in Central Mexico: from Sierra Madre Occidental to Mexican Volcanic Belt. *Geology* **27**, 303–6,

Ferrusquía-Villafranca I (1987) Reubicación geocronológica del Conglomerado Guanajuato basada en nuevos mamíferos (resumen). In *El Programa, Resúmenes y Guía de Excursión del Simposio Sobre la Geología de la región de la Sierra de Guanajuato, Guanajuato*, pp. 21–23. Mexico City: Universidad Nacional Autónoma de México, Instituto de Geología.

Gottsmann J and Martí J (2008) *Caldera Volcanism: Analysis, Modelling and Response*. Amsterdam: Elsevier.

Gross WH (1975) New ore discovery and source of silver-gold veins, Guanajuato, Mexico. *Economic Geology* **70**, 1175–89.

Guiza R, Rendón C and Baltierra-G JJ (1949) *Estudio Geológico del Distrito Minero de Guanajuato, Gto. (zona de la Veta Madre)*. Mexico City: Instituto Nacional para la Investigación de Recursos Minerales.

Henry CD and Aranda-Gómez JJ (1992) The real southern Basin and Range; mid- to late Cenozoic extension in Mexico. *Geology* **20**, 701–4.

INEGI (2023) Cartas topográficas 1:50:000: web site https://www.inegi.org.mx/programas/topografia/50000/.

International Commission on Stratigraphy (2013) *Stratigraphic Guide – An Abridged Version*. In *International Stratigraphic Guide – An Abridged Version*, eds MA Murphy and A Salvador; revised by WE Piller and MP Aubry. 2013–2022 online publication. Available at https://stratigraphy.org/guide/index.html (accessed 23 February 2024).

Lapierre H, Ortiz E, Abouchami W, Monod O, Coulon C and Zimmermann JL (1992) A crustal section of an intra-oceanic island arc: the Late Jurassic–Early Cretaceous Guanajuato magmatic sequence, central Mexico. *Earth and Planetary Science Letters* **108**, 61–77.

Lipman PW (1997) Subsidence of ash-flow calderas: relation to caldera size and magma-chamber geometry. *Bulletin Volcanologique* **59**, 198–218.

Mahood GA (1980) Geological evolution of a Pleistocene rhyolitic center – Sierra La Primavera, Jalisco, Mexico. *Journal of Volcanology and Geothermal Research* **8**, 199–230.

Mango H, Zantop H and Oreskes N (1991) A fluid inclusion and isotope study of the Rayas Ag-Au-Cu-Pb-Zn Mine, Guanajuato, México. *Economic Geology* **86**, 1554–61.

Martí J (1991) Caldera-like structures related to Permo-Carboniferous volcanism at the Catalan Pyrinees (NE Spain). *Journal of Volcanology and Geothermal Research* **45**, 173–86.

Martí J, Groppelli G and Brum da Silveira A (2018) Volcanic stratigraphy: a review. *Journal of Volcanology and Geothermal Research* **357**, 68–91.

Martí J, Planagumà LL, López-Pla A and López-López JA (2023) La caldera volcànica d'Estac. Itineraris, Georuta d'Estac. *Generalitat de Catalunya, Parc Natural de l'Alt Pirineu*, Ajuntament de Soriguera, 30 p.

Martí J, Rodríguez C, Aguirre-Díaz GJ and Solari L (2024) Geochronology and geochemistry of the Greixer rhyolitic caldera complex: Implications on Permo-Carboniferous magmatism (South-Central Pyrenees, NE Spain). *Lithos* **470–471**, 107524. https://doi.org/10.1016/j.lithos.2024.107524; www.elsevier.com/locate/lithos.

Martínez-Reyes J (1992) Mapa geológico de la Sierra de Guanajuato con resumen de la geología de la Sierra de Guanajuato. *Cartas geológicas y mineras, Universidad Nacional Autónoma de México, Instituto de Geología*, 8, escala 1:100,000.

McDowell FW and Clabaugh SE (1979) Ignimbrites of the Sierra Madre Occidental and their relation to the tectonic history of western Mexico. *Geological Society of America Special Paper* **180**, 113–24.

Miranda-Avilés R, Puy-Alquiza MJ, Omaña L and Loza-Aguirre I (2016) Los depósitos clásticos pos-Laramide de la Sierra de Guanajuato: Implicaciones de su composición en la evolución tectono-sedimentaria y paleogeográfica. *Estudios Geológicos* **72**, e058. http://dx.doi.org/10.3989/egeol.42480.417.

Molina-Zúñiga F, Marti J and Aguirre-Díaz GJ (2014) Stratigraphy and structure of the Cañas Dulces caldera, Costa Rica. *Geological Society of America Bulletin* **126**, 1465–80. http://doi.org/10.1130/B31012.1.

Monod O, Lapierre H, Chiodi M, Martinez J, Calvet P, Ortiz E and Zimmermann JL (1990) Reconstitution d'un arc insulaire intra-océanique au Mexique central: la séquence volcanoplutonique de Guanajuato (Crétacé inférieur). *Comptes Rendus de l'Académie des Sciences. Série 2, Mécanique, Physique, Chimie, Sciences de l'univers, Sciences de la Terre* **310**, 45–51.

Nieto-Samaniego ÁF, Alaniz-Álvarez SA and Camprubí A (2007) Mesa Central of México: stratigraphy, structure, and Cenozoic tectonic evolution. *Geological Society of America Special Paper* **422**, 41–70.

Nieto-Samaniego AF, Báez-López JA, Levresse G, Alaníz-Álvarez SA, Ortega-Obregón C, López-Martínez M and Solé-Viñás J (2016) New stratigraphic, geochronological, and structural data from the southern Guanajuato Mining District, México: Implications for the caldera hypothesis. *International Geology Review* **58**, 246–62.

Nieto-Samaniego AF, Macías-Romo C and Alaniz-Alvarez SA (1996) Nuevas edades isotópicas de la cubierta volcánica cenozoica de la parte meridional de la Mesa Central, México. *Revista Mexicana de Ciencias Geológicas* **13**, 117–22.

Nixon GT (1982) The relationship between Quaternary volcanism in central Mexico and the seismicity and structure of subducted ocean lithosphere. *Geological Society of America Bulletin* **93**, 514–23.

Orozco-Villaseñor FJ (2014) Mineralogía y génesis del "clavo de Rayas" de la zona central de la Veta Madre de Guanajuato. Tesis doctorado Posgrado Ciencias de la Tierra, Universidad Nacional Autónoma de México, 240 p. Published thesis.

Ortega-Gutiérrez F, Elias-Herrera M and Dávalos-Elizondo MA (2008) On the nature and role of the lower crust in the volcanic front of the Trans-Mexican Volcanic Belt and its fore-arc region, southern and central Mexico. *Revista Mexicana de Ciencias Geológicas* **25**, 346–64.

Ortiz-Hernández LE, Chiodi M, Lapierre H, Monod O and Calvet PH (1990) El arco intraoceánico alóctono (Cretácico Inferior) de Guanajuato: características petrográficas, geoquímicas, estructurales e isotópicas del complejo filoniano y de las lavas basálticas asociadas; implicaciones geodinámicas. *Revista Mexicana de Ciencias Geológicas* **9**, 125–45.

Paton C, Woodhead JD, Hellstrom JC, Hergt JM, Greig A and Maas R (2010) Improved laser ablation U-Pb zircon geochronology through robust downhole fractionation correction. *Geochemistry, Geophysics, Geosystems* **11**, Q0AA06.

Petrus JA and Kamber BS (2012) VizualAge: a novel approach to laser ablation ICP-MS U-Pb geochronology data reduction. *Geostandards and Geoanalytical Research* **36**, 247–70.

Puy-Alquiza MJ, Miranda-Avilés R, Cruz-Cruz M, Pérez-Arbizu O, Vega-González M and Ana-Zanor G (2014) Geochemistry and depositional environment of the Losero Formation in the Mesa Central, México. *Boletín de la Sociedad Geológica Mexicana* **66**, 413–30.

Puy-Alquiza MJ, Miranda-Avilés R, Loza-Aguirre I, Li Y, García-Barragán JC and Zanor GA (2017) Facies analysis, stratigraphic architecture and depositional environments of the Guanajuato conglomerate in the Sierra de Guanajuato, Mexico. *Boletín de la Sociedad Geológica Mexicana* **69**, 385–408.

Quintero O (1992) Geología de la región de Comanja, estados de Guanajuato y Jalisco. *Revista Mexicana de Ciencias Geológicas* **10**, 6–25.

Randall JA, Saldaña E and Clark KF (1994) Exploration in a volcano-plutonic center at Guanajuato, México. *Economic Geology* **89**, 1722–51.

Saura E, Martí J, Cirés J and Clariana P (2025) The Permo-Carboniferous Basins of the Catalan Pyrenees (NE Iberia): An Example of Interacting Tectonics and Collapse Calderas. *Tectonics* **44**, e2025TC008924. https://doi.org/10.1029/.

Sedlock RL, Ortega GF and Speed RC (1993) Tectonostratigraphic terranes in Mexico and tectonic evolution of Mexico. *Geological Society of America Special Paper* **278**, 153.

Servicio Geológico Mexicano (2023) Cartas Geológicas Mineras: web site https://www.sgm.gob.mx/CartasDisponibles/.

Siebe C, Macías JL and Aguirre-Díaz GJ (2006) Neogene-Quaternary continental margin volcanism: A perspective from Mexico. *Geological Society of America Special Paper* **402**, 329. https://doi.org/10.1130/0-8137-2402-3.

Sláma J, Košler J, Condon D, Crowley J, Gerdes A, Hanchar J, Horstwood M, Morris G, Nasdala L, Norberg N, Schaltegger U, Schoene B, Tubrett M and Whitehouse MJ (2008) Plešovice zircon—a new natural reference material for U–Pb and Hf isotopic microanalysis. *Chemical Geology* **249**, 1–35. https://doi.org/10.1016/j.chemgeo.2007.11.005.

Solari LA, González-León CM, Ortega-Obregón C, Valencia-Moreno M and Rascón-Heimpel MA (2018) The Proterozoic of NW Mexico revisited: U–Pb geochronology and Hf isotopes of Sonoran rocks and their tectonic implications. *International Journal of Earth Sciences* **107**, 845–61.

Stewart JH (1978) Basin and range structure in western North America: a review. *Geological Society of America Memoir* **152**, 1–30.

Suñe-Puchol I, Aguirre-Diaz GJ, Davila Harris P, Miggins D, Pedrazzi D, Costa A, Ortega-Obregón C, Lacan P, Hernández W and Gutiérrez E (2019a) The Ilopango caldera complex, El Salvador: Origin and early ignimbrite-forming eruptions of a graben/pull-apart caldera structure. *Journal of Volcanology and Geothermal Research* **371**, 1–19. https://doi.org/10.1016/j.jvolgeores.2018.12.004.

Suñe-Puchol I, Aguirre-Diaz GJ, Davila Harris P, Miggins D, Pedrazzi D, Costa A, Ortega-Obregón C, Lacan P, Hernández W and Gutiérrez E (2019b) The Ilopango caldera complex, El Salvador: Stratigraphic revision of complete eruptive sequence and recurrence of large explosive eruptions. *Journal of Volcanology and Geothermal Research* **374**, 100–19. https://doi.org/10.1016/j.jvolgeores.2019.02.011.

Tristán-González M, Aguirre-Díaz GJ, Labarthe-Hernández G, Torres-Hernández JR and Bellon H (2009) Post-Laramide and pre-Basin and range deformation and implications for Paleogene (55–25 Ma) volcanism in central Mexico: a geological basis for a volcano-tectonic stress model. *Tectonophysics* **471**, 136–52.

Tristán-González M, Labarthe-Hernández G, Aguirre-Díaz GJ and Aguillón-Robles A (2008) Tectono-volcanic control of fissure type vents for the 28 Ma Panalillo ignimbrite in the Villa de Reyes Graben, San Luis Potosí, México. *IOP Conference Series: Earth and Environmental Science* **3**, 012026.

Ubach-Cozatl ME (2023) Brechas co-ignimbríticas de rezago como indicadores de proximidad a conductos de la caldera graben de Guanajuato. Tesis Profesional, Ciencias de la Tierra, Facultad de Ciencias, UNAM, 869 p. Published thesis.

Ubach-Cozatl ME and Aguirre-Díaz GJ (2023) Brechas co-ignimbríticas líticas de rezago de la caldera tipo graben de Guanajuato. *Reunión Anual Unión Geofísica Mexicana 2023*, Resumen 0072 - Vulcanología. https://www.raugm.org.mx/resumenes/sessions/abstract.php?abstractID=72&source=session.

Vassallo LF (2018) Regional geological setting of Guanajuato silver-gold deposits and quantitative petrophysical assessment of their hydrothermal alteration, Guanajuato, México. *Ore Geology Reviews* **101**, 502–19.

Vermeesch P (2018) IsoplotR: a free and open toolbox for geochronology. *Geoscience Frontiers* **9**, 1479–93.

Walker GPL (1985) Origin of coarse lithic breccias near ignimbrite-source vents. *Journal of Volcanology and Geothermal Research* **25**, 157–71.

Wandke A and Martínez J (1928) The Guanajuato mining district, Guanajuato, Mexico. *Economic Geology* **23**, 1–44.

Wiedenbeck M, Allé PF, Griffin WL, Meier M, Oberli F, Von Quadt A, Roddick J and Spiegel W (1995) Three natural zircon standards for U-Th-Pb, Lu-Hf, trace element and REE analyses. *Geost News* **19**, 1–23.